Nucleic Acids Research, 2017 **1**
doi: 10.1093/nar/gkx194

New inhibitor targeting human transcription factor HSF1: effects on the heat shock response and tumor cell survival

Nuria Vilaboa[1,2], Alba Boré[1,2], Francisco Martin-Saavedra[1,2], Melanie Bayford[3], Natalie Winfield[3], Stuart Firth-Clark[3], Stewart B. Kirton[4] and Richard Voellmy[5,*]

[1]Hospital Universitario La Paz-IdiPAZ, 28046 Madrid, Spain, [2]CIBER de Bioingenieria, Biomateriales y Nanomedicina, CIBER-BBN, Madrid, Spain, [3]Domainex Ltd, Chesterford Research Park, Little Chesterford, Saffron Walden, Essex CB10 1XL, UK, [4]University of Hertfordshire, Hatfield, Hertfordshire, AL10 9AB, UK and [5]HSF Pharmaceuticals SA, 1814 La Tour-de-Peilz, Switzerland

Received September 19, 2016; Revised February 20, 2017; Editorial Decision March 10, 2017; Accepted March 13, 2017

ABSTRACT

Comparative modeling of the DNA-binding domain of human HSF1 facilitated the prediction of possible binding pockets for small molecules and definition of corresponding pharmacophores. *In silico* screening of a large library of lead-like compounds identified a set of compounds that satisfied the pharmacophoric criteria, a selection of which compounds was purchased to populate a biased sub-library. A discriminating cell-based screening assay identified compound 001, which was subjected to systematic analysis of structure–activity relationships, resulting in the development of compound 115 (I_{HSF}115). I_{HSF}115 bound to an isolated HSF1 DNA-binding domain fragment. The compound did not affect heat-induced oligomerization, nuclear localization and specific DNA binding but inhibited the transcriptional activity of human HSF1, interfering with the assembly of ATF1-containing transcription complexes. I_{HSF}115 was employed to probe the human heat shock response at the transcriptome level. In contrast to earlier studies of differential regulation in HSF1-naïve and -depleted cells, our results suggest that a large majority of heat-induced genes is positively regulated by HSF1. That I_{HSF}115 effectively countermanded repression in a significant fraction of heat-repressed genes suggests that repression of these genes is mediated by transcriptionally active HSF1. I_{HSF}115 is cytotoxic for a variety of human cancer cell lines, multiple myeloma lines consistently exhibiting high sensitivity.

INTRODUCTION

The stress or heat shock response (HSR) is a key mechanism for maintaining cellular proteostasis under conditions of heat or other proteotoxic stress. The response encompasses increased expression of so called heat shock proteins (HSPs), molecular chaperones that reduce aggregation of misfolded proteins and promote their refolding or disposal (1,2). Activation of the HSR is triggered by protein damage that occurs in cells exposed to excessive but non-lethal heat or to chemicals or other conditions that cause proteins to become denatured (3,4).

The master regulator of the mammalian HSR is heat shock transcription factor 1 (HSF1) (5,6). In the absence of a stress, HSF1 is predominantly present in cells in an inactive, hetero–oligomeric complex comprising HSP90 and co-chaperones (7–10). Several additional proteins are known or inferred to bind HSF1 or HSF1 complex, including CHIP (11), HDAC6 (12,13), p97/VCP (12,13), DAXX (14), 14-3-3 (15), FILIP-1L (16) and HSBP1 (17). More recently, this list was expanded considerably by Fujimoto *et al*. and, most notably, now includes ATF1 and RPA1, which proteins interact with the HSF1 DNA-binding domain (18,19).

Stress-mediated activation of HSF1 and maintenance of the factor in an active form involves a multitude of events. An early event is the dissociation of HSP90 or HSP90 complex from the inactive HSF1 complex and the consequential homo-trimerization of HSF1 (7,20). HSF1 trimers are capable of specific DNA-binding. However, whether they are also transactivation-competent appears to depend in part on whether they are capable of escaping re-association with HSP90 and/or HSP70 (21,22). Transcriptional activity of HSF1 will also depend on DAXX as well as on its phosphorylation status (14,23–25). Recruitment of HSF1 to target promoters in response to a stress is mediated by ATF1/CREB (19). ATF1/CREB regulates the stress-induced HSF1 transcription complex

*To whom correspondence should be addressed. Tel: +41 21 534 0260; Email: rvoellmy@hsfpharma.com

that includes BRG1 chromatin-remodeling complex and p300/CBP. The former complex promotes an active chromatin state in the promoters, whereas p300/CBP accelerates the shutdown of HSF1 DNA-binding activity as well as stabilizes HSF1 against proteasomal degradation during recovery from stress (19,26). This shutdown is counteracted by SIRT1-mediated deacetylation (27).

Beyond regulation of typical HSR genes such as *HSP* genes, activated HSF1 influences the activities of genes related to a variety of basic cellular processes. This HSF1-induced program may facilitate oncogenic transformation and maintenance of a malignant phenotype (28–33). Dai *et al*. demonstrated that genetic elimination of HSF1 protects mice from tumors induced by mutations in the *RAS* oncogene or a hot spot mutation in tumor suppressor gene *P53* and that ablation of HSF1 by RNA interference is cytotoxic to various cancer cell lines (31). Work by others in different *in vitro* and *in vivo* cancer models permitted generalization of these findings (34–37). Consistent with the dependence of many cancers on HSF1 activity is the observation of elevated nuclear levels of HSF1 in a high proportion of breast cancer samples from *in situ* and invasive breast carcinomas obtained from 1841 study participants (38). High levels of HSF1 were correlated with poor survival. A subsequent study found high levels of nuclear HSF1 to be common in a wide range of cancers (30). These findings propound HSF1 as a promising new cancer therapeutic target.

A specific inhibitor that directly targets HSF1 could be expected to be a useful tool for better understanding mechanisms of regulation of HSF1 activity as well as for investigating the consequences of acute interruption of HSF1 function. Furthermore, such an inhibitor may be developed into a therapeutic agent that may prove valuable in the therapy of multiple cancer types and other conditions dependent on HSF1 activity. To date, no such specific inhibitor has been developed. An inhibitory nitropyridine compound named KRIBB11 has been described that may interact with HSF1 or a complex comprising HSF1 (39). However, the molecule lacks specificity, belonging to a class of compounds that are effective inhibitors of reverse transcriptases (40). It is noted that an RNA aptamer has been reported that is capable of inhibiting HSF1 binding to its target genes in transfected human cells (41). Herein we report on the *de novo* development of a drug-like inhibitor that targets human HSF1 and describe its mechanism of inhibition as well as biological consequences of exposure to this inhibitor.

MATERIALS AND METHODS

Chemical compounds

Details of syntheses are provided under Supplemental Methods, Supporting Information. All compounds were characterized by liquid chromatography mass spectrometry (LCMS) and ^{1}H nuclear magnetic resonance (NMR). Compounds 001 and 004 were obtained from AKos Consulting & Solutions GmbH and Ambinter, respectively.

Plasmids and subcloning

A fragment containing *Renilla* luciferase (*RLUC*) coding sequences and SV40 polyA sequences was polymerase chain reaction (PCR)-amplified from *phRL-CMV* (Promega) using primers 5′-TCACTATAAGCTTGCCACCATGG-3′ and 5′-CCTGGAAGCTTATCGATTTTACCA-3′, digested with HindIII and inserted into the HindIII site of *pSP72-Hsp70B* (42). The resulting construct was designated *pHsp70B-Ren*. A firefly luciferase (*FLUC*) gene flanked by a LEXA binding site-containing promoter and SV40 polyA sequences was PCR-amplified from *pLexA-Luc* (21) using primers 5′-ATCTTATGGTACCGTAACTGAGC-3′ and 5′-CAAGGGTACCGGTCGACGGAT-3′, digested with KpnI and inserted into the KpnI site of *pHsp70B-Ren*. Resulting construct *pHsp70B-Ren/LexA-Luc* contained the latter *HSP70B-RLUC* and *LEXA-FLUC* genes arranged in the same orientation. *pLexAHSF1wt* is a *pcDNA3.1(+)*-derived plasmid (Invitrogen) that encodes a chimeric HSF1 containing the first 87 codons of LEXA linked in frame to codon 79 of human HSF1 (43,44). In the version used herein, HSF1 amino acids 183–203 were replaced by KQLLQQILNLIVNILNQSKLI. To prepare *pGSLink-HSF1WT*, an internal NcoI site in the HSF1-coding sequence was destroyed by QuickChange site-directed mutagenesis of *pcDNA3.1(+)*-derived *pHSF1WT*, using primers 5′-CCTGCCAGCCCAATGGCCTCCCC-3′ and 5′-GGGGAGGCCATTGGGCTGGCAGG-3′. The resulting construct served as template for PCR amplification using primers 5′-GCTTGTTAACCATGGATCTGC-3′ and 5′-TGTCCCGGGAGACAGTGGGGTCCTTGGCTTT-3′. The PCR product was digested with NcoI and XmaI and inserted into the NcoI/XmaI sites of *pGSLink* (45). To prepare *pGSLink-HSF1DBD*, the HSF1 DNA-binding domain-encoding sequence of HSF1 was PCR-amplified from *pHSF1WT* using primers 5′-GCTTGTTAACCATGGATCTGC-3′ and 5′-TGTCCCGGGATCTTTATGTC-3′. The PCR product was digested with NcoI and XmaI and inserted into the NcoI/XmaI sites of *pGSLink*. To obtain *pCTF-HSF1WT,* a plasmid encoding a FLAG peptide fused to the C-terminus of HSF1, the HSF1-coding sequence was PCR-amplified from *pHSF1WT* using primers 5′-GTTAGGTACCATGGATCTGCCCGTGG-3′ and 5′-GTTAGGTACCGGAGACAGTGGGGTCCTTG-3′. The PCR product was digested with KpnI and inserted into the KpnI site of *pCMV-(DYKDDDDK)-C* (Clontech). All subcloning and mutagenesis steps were monitored by restriction analysis and nucleotide sequencing.

Cell culture, transfection and isolation of cell lines

Human HeLa (ATCC CCL-2), Saos-2 (ATCC HTB-85), MG-63 (ATCC CRL-1427), U-2 OS (ATCC HTB-96), HepG2 (ATCC HB-8065), T-47D (ATCC HTB-133), BT-474 (ATCC HTB20), A549 (ATCC CCL185), MDA-MB-453 (ATCC HTB131), sNF02.2 (ATCC CRL-2885) and sNF96.2 (ATCC CRL-2884) cells were cultured in Dulbecco's modified Eagle's medium (DMEM; Lonza). Human THP-1 (ATCC TIB202), NCI-H3122, NCI-H2228 (ATCC CRL-5935), NCI-H1975 (ATCC CRL-5908), NCI-H460

(ATCC HTB177), HCC1143 (ATCC CRL-2321), MDA-MB-231 (ATCC HTB26), IM-9 (ATCC CCL159), MNNG-HOS (ATCC CRL1547), A673 (ATCC CRL1598), U266B1 (ATCC TIB-196), RPMI 8266 (ATCC CCL-155), MM.1R (ATCC CRL-2975) and MM.1S (ATCC CRL2974) cells were cultured in RPMI-1640 medium (Lonza). Human BT-20 cells (ATCC HTB19), CAMA-1 cells (ATCC HTB-21) and normal human embryonic WI-38 fibroblasts (ATCC CCL-75) were cultured in Eagle's minimum essential medium (EMEM; Lonza). Human MCF-7 cells (ATCC HTB-22) were cultured in EMEM supplemented with 1% non-essential amino acids. Human SK-N-SH cells (ATCC HTB11) were cultured in DMEM supplemented with 1.25 mM HEPES, pH 7.3. Human SK-OV-3 (ATCC HTB77), OV56 (ECACC 96020759) and PEA1 (ECACC 10032306) cells were cultured in RPMI-1640 supplemented with 1 mM sodium pyruvate. Human PC-3 cells (ATCC CRL-1435) were cultured in F-12 Coon's modified medium (Lonza). DMEM, EMEM and RPMI media were supplemented with 10% (v/v) fetal bovine serum. F-12 Coon's modified medium was supplemented with 7% (v/v) fetal bovine serum. All media were supplemented with 10 U/ml penicillin and 0.01 mg/ml streptomycin. Cells were maintained in a humidified 5% CO_2 atmosphere at 37°C. Except for NCI-H3122 which was from NCI, and OV56 and PEA1 which were from ECACC, all the above-mentioned cell lines were from ATCC. To obtain cell line Z74 containing *HSP70B-RLUC*, *LEXA-FLUC* and *CMV-LEXA-HSF1* genes, HeLa cells were co-transfected with *pHsp70B-Ren/LexA-Luc* and *pLexAHSF1* (5:1 molar ratio). To obtain cell line CTF135 harboring a FLAG-tagged version of the *CMV-HSF1* gene, HeLa cells were co-transfected with *pCTF-HSF1WT* and a *pcDNA3.1-derived* vector expressing a neomycin resistance gene (42) (4:1 molar ratio). Cell lines were isolated after selection with 600 μg/ml G418. HSF2-deficient cell line HF73 was prepared by transfection of HeLa cells with equal amounts of the three plasmids of the human HSF2 sgRNA CRISPR/Cas9 All-in-One Lentivector set of Applied Biological Materials. Cell lines we isolated after selection with 1.3 μg/ml puromycin. All transfections employed Lipofectamine reagent (Invitrogen).

Measurement of reporter gene activities in Z74 cells

Z74 cells (1×10^4) were seeded in 96-well plates and cultured for 24 h. At that time, cultures were pre-incubated for 2 h with a compound to be tested or vehicle, heated, typically at 43°C, for 30 min in a thermostatically controlled water bath and then incubated for an additional 6 h at 37°C. FLUC and RLUC activities were determined using the Dual-Glo™ Luciferase Assay System (Promega). Luciferase light counts were detected in a Wallac Microbeta Trilux-1450 Luminometer (Perkin–Elmer).

Protein purification and surface plasmon resonance (SPR) analysis

Escherichia coli BL21(DE3) Codon Plus cells (Stratagene/Agilent Technologies) were transformed with *pGSLink-HSF1WT* or *pGSLink-HSF1DBD*. Expression of His-tagged proteins induced by 0.1 mM isopropyl-1-thio-β-D-galactopyranoside was for 2.5 h (HSF1WT) or 5 h (HSF1DBD) at 20°C. Cells were harvested by centrifugation, re-suspended in lysis buffer (20 mM Tris–HCl, pH 7.9, 300 mM NaCl) supplemented with a protease inhibitor cocktail (Complete, Roche Applied Science) and disrupted on ice using a sonicator. Soluble fractions were purified on 5-ml HisTrap FF columns in an ÄKTA Prime Plus FPLC system (both from GE Healthcare Life Sciences) at a flow rate of 1 ml/min. Columns were pre-equilibrated with lysis buffer. Following washes with lysis buffer containing 4 mM imidazole, proteins were eluted with lysis buffer containing 400 mM imidazole. Purified HSF1WT was dialyzed against lysis buffer. The proteins were concentrated to 10 mg/ml using concentrator devices (Vivaspin, GE Healthcare Life Sciences) with a 10 kDa (HSF1WT) or a 3 kDa (HSF1DBD) cut-off, respectively. Purity of the proteins was determined by Coomassie blue staining of sodium dodecyl sulphate-polyacrylamide gel electrophoresis (SDS-PAGE) gels. Surface plasmon resonance (SPR) assays were performed using a Biacore 3000 instrument (Biacore AB). HSF1WT and HSF1DBD proteins were immobilized on CM5 sensor chips (Biacore) using a standard amine coupling procedure, after activation of surface carboxyl groups by the addition of a mixture of N-hydroxysuccinimide and 1-ethyl-3-(3-diaminopropyl)carbodiimide. HSF1WT and HSF1DBD proteins were immobilized until reaching coupling densities of 12 and 3.5 ng/mm^2, respectively. Immediately before SPR assays, test compounds were dissolved at 10 mM in dimethyl sulfoxide (DMSO) and then diluted into running buffer (10 mM sodium phosphate, pH 7.5, 150 mM sodium chloride, 0.005% Tween 20, 5% DMSO). Interaction assays were performed at 25°C using a flow rate of 50 μl/min. A reference cell was used to subtract possible nonspecific binding to the chip surface. Regeneration was with 2 M NaCl.

Analysis of DNA–protein interactions

HeLa cells (1.75×10^6) were seeded in 100 mm dishes and cultured for 24 h. At that time, the cells were pre-exposed to indicated doses of compounds or vehicle for 2 h and then heat-treated as detailed above. For electrophoretic mobility gel shift analysis, whole cell extracts were prepared immediately after heat treatment as previously described (43,44). Protein concentration in cell extracts was determined by a Bradford-based protein assay (Bio-Rad Laboratories Inc.). Partially complementary oligonucleotides 5′-GCCTCGAATGTTCGCGAAGTTT-3′ and 5′-CGAAACTTCGCGAACATTCGAG-3′ were annealed to obtain a probe fragment containing an heat shock element (HSE) sequence (46). The fragment was labeled with [α-32P]dCTP as earlier reported (47). For typical binding reactions, 5 μl cell extract containing 15 μg proteins were combined with 10 μl 'Kingston' buffer (4 mM $MgCl_2$, 0.24 mM ethylenediaminetetraacetic acid (EDTA), 24% (v/v) glycerol, 24 mM HEPES, pH 7.9), 2 μl poly(dI-dC) at 1 mg/ml and 1 μl water. After a 15-min pre-incubation in ice, 2 μl of the labeled probe (∼10 000 cpm) were added, and the reaction was incubated for 15 min at room temperature (RT). Reactions were electrophoresed on 4.5% native polyacrylamide gels. Dried gels were subjected to autoradiography. For chromatin immunoprecipitation (ChIP)

assays, HeLa cells (4.4×10^6) were seeded in 150 mm dishes, cultured for 24 h and then treated as described above. Immediately after heating, cells were fixed with 1% formaldehyde for 10 min at RT. ChIP assays were performed using the ChIP-IT Express Magnetic Chromatin Immunoprecipitation kit (Active Motif). Briefly, chromatin was sheared by enzymatic digestion and immunoprecipitated using a cocktail of rat anti-human HSF1 monoclonal antibodies (Clones 4B4, 10H4, 10H8; Thermo-Fisher Scientific) or, for control, a rat anti-F4/80 monoclonal antibody (BD Biosciences). Following overnight incubation at 4°C in a rotator, immunoprecipitates were collected using magnetic protein G beads. Chromatin was reverse-cross-linked, and DNA purified and subjected to real-time quantitative PCR (qPCR) to detect recruitment of HSF1 to the *HSPA1A* gene promoter. Specific oligonucleotide primers were 5′-ATTGGTCCAAGGAAGGCTGG-3′ and 5′-CTCAGGCTAGCCGTTATCCG-3′. qPCR was performed using LightCycler FastStart DNA Master SYBR Green I and a LightCycler instrument (both from Roche Applied Science). Samples of not-immunoprecipitated chromatin were used as input controls for PCR amplification.

Analysis of differential gene expression by reverse transcription (RT) and qPCR

Z74 cells (3×10^5) were seeded in 6-well plates and cultured for 24 h. At that time, cells were pre-exposed to test compound or vehicle for 2 h and then heat-treated as described above. After a further incubation for 1 h at 37°C, total RNA was prepared using TRI Reagent (Molecular Research Center, Inc.), following the manufacturer's instructions. To quantify the levels of *RLUC, HSPA1A, HSPA7* and *DUSP1* mRNA, cDNA was prepared from total RNA using Transcriptor reverse transcriptase and an anchored-oligo $(dT)_{18}$ primer (both from Roche Applied Science). qPCR was performed as described in the preceding section. Quantitative expression values were extrapolated from standard curves, and were normalized to *β2-microglobulin* (*B2M*) values. Specific oligonucleotide primers were: *RLUC*: 5′- ATGGGATGAATGGCCTGATA-3′ (F), 5′-TGTTGGACGACGAACTTCAC-3′ (R); *DUSP1*: 5′ AGGCCATTGACTTCATAGACTCC-3′ (F) and 5′-TGGGAGAGATGATGCTTCGC-3′(R); *B2M*: 5′-CCAGCAGAGAATGGAAAGTC-3′ (F), 5′-GATGCTGCTTACATGTCTCG-3′ (R). Levels of *HSPA1A* and *HSPA7* mRNA were estimated using the Hs_HSPA1A_1_SG QuantiTect Primer Assay and the Hs_HSPA7_FAM_1 QuantiFast Probe Assay, respectively (both from Qiagen). In some experiments, cDNA was prepared using *RLUC* (R) and *B2M* (R) primers. To quantify the levels of *DNAJA4*, *DNAJB1*, *DNAJB6, DNAJC28, EGR1, FOSB, HIST1H1A, HIST1H1B, HIST1H1C*, *HIST1H1E*, *HIST1H2AI*, *HSPA1L*, *HSPA6, IER5*, *JUN*, *TADA1* and *VHLL* mRNA, cDNA was prepared from total RNA using the High-Capacity RNA-to-cDNA™ Kit (Life Technologies). qPCR was performed using TaqMan Gene Expression Assays (Life Technologies, see Supplementary Table S1, Supporting Information, for Assay IDs) and TaqMan Gene Expression Master Mix. qPCR reactions were run in an 7900HT Fast Real-Time PCR System (Applied Biosystems). Sequence Detector Software 2.4 (Applied Biosystems) was used for data analysis. A threshold cycle (CT) value was determined from a log-linear plot of the PCR signal versus the cycle number. All data were converted to the linear form by 2^{-CT} determination. *B2M* (Assay ID Hs00187842_m1), *GUSB* (Assay ID Hs00939627_m1) and *HPRT1* (Assay ID Hs02800695_m1) were used as endogenous controls.

Microarrays analysis of differential gene expression

HeLa cells (1.75×10^6) were seeded in 100 mm dishes and cultured for 24 h. The cells were then pre-exposed to test compound or vehicle for 2 h and heat-treated as described above. After a further incubation for 1 h at 37°C, total RNA was prepared using the RNeasy Mini Kit (Qiagen) and processed using GeneChip WT PLUS Reagent kit, hybridized with GeneChip Human Gene 2.0 ST Array and scanned with a GeneChip scanner 3000 7G (all from Affymetrix). Raw data were normalized and gene levels analyzed using the RMA algorithm (Affymetrix Expression Console). For each experimental condition, three (HeLa) or five (HF73) RNA replicates corresponding to independent experiments were processed and analyzed. Fold changes between experimental conditions were calculated as ratios of means of gene expression signals. Genes with $\geq$1.400- or $\leq$ 0.714-fold changes were included for further analysis. Gene ontology analyses were performed using the Database for Annotation, Visualization and Integrated Discovery (DAVID; http://david.abcc.ncifcrf.gov) (48). Conclusions drawn from microarray experiments regarding type of regulation were corroborated by RT-qPCR analysis for a representative number of genes (Supplementary Table S1, Supporting Information).

Immunoblotting (WB) experiments

Cellular proteins were extracted with lysis buffer (50 mM Tris–HCl, pH 8.0, 150 mM NaCl, 1% NP-40, 0.5% deoxicholate, 0.1% SDS, 1 mM dithiothreitol (DTT), 1 mM Na_3VO_4, 1 mM phenylmethylsulfonyl fluoride (PMSF)) supplemented with a protease inhibitor cocktail (Complete). In some experiments, whole cell extracts (43,44) were used to assess levels of HSF1. Protein concentration in cell lysates was determined by a Bradford-based protein assay. A total of 25 μg of proteins were resolved by SDS-PAGE, transferred to a PVDF membrane and analyzed by immunoblotting using mouse anti-human HSP72 monoclonal antibody C92F3A-5, rabbit anti-human HSF1 polyclonal antibody SPA-901 or rat anti-mouse HSF2 monoclonal antibody SPA-960 (all from Enzo). A mouse anti-human GAPDH monoclonal antibody 9484 (Abcam) was used as a loading control. HSF1 oligomerization was assessed using amine-specific cross-linker ethylene glycol bis-succinimidyl succinate (EGS) (Pierce). Whole cell extract (50 μg) prepared as previously described (43,44) was incubated with 0.5 mM EGS for 30 min at RT. The cross-linking reaction was quenched by the addition of 50 mM glycine/0.025 mM Tris, pH 7.5 and incubation for 15 min at RT. Proteins were fractionated through a 6% SDS-PAGE

gel and analyzed by immunoblotting using anti-HSF1 antibody SPA-901.

shRNA knockdown

Z74 cells (8×10^4) were seeded in 12-well plates and cultured for 24 h. At that time, the cells were transduced with HSTF1 shRNA (h) or control shRNA lentiviral particles-A (both from Santa Cruz Biotechnologies) at multiplicity of infection (MOIs) of 3, using 5 μg/ml polybrene. One day later, medium containing lentiviral particles was replaced with fresh medium, and cells were cultured for another day. Thereafter, cells were incubated for one day in medium containing 1.3 μg/ml puromycin and then trypsinized and seeded at 1×10^4 cells/well in 96-well plates. At this time, aliquots of cells were harvested, extracted in lysis buffer (see the preceding section) and levels of HSF1 and LEXA-HSF1 assessed by WB. LEXA-HSF1 was detected using rabbit anti-LexA DNA Binding Region polyclonal antibody 14553 (Abcam). After one day of further incubation, cells were heated at 43°C for the indicated periods of time (or not) and then post-incubated for 6 h at 37°C. FLUC and RLUC activities were measured as described above.

Immunoprecipitations

CTF135 cells (4.4×10^6) cells were seeded in 150 mm dishes, cultured for 24 h, exposed to test compound or vehicle for 2 h and then heat-treated as described above. Cells were extracted on ice with lysis buffer (50 mM HEPES-KOH, pH 8.0, 100 mM KCl, 2 mM EDTA, 0.1% NP40, 10% glycerol) supplemented with 1 mM DTT, 1 mM PMSF, 0.25 mM sodium orthovanadate, 50 mM β-glycerolphosphate, 10 mM NaF, 5 nM okadaic acid, 5 nM calyculin A and protease inhibitor cocktail (Complete). Cells were lysed by three cycles of rapid freezing (dry ice-ethanol bath) and thawing (37°C water bath). Cell debris was then removed from cell lysates by centrifugation at 16 000 *g* for 20 min at 4°C. Protein concentrations of extracts were determined using the protein assay reagent of Bio-Rad and were equalized prior to further analysis. Aliquots of extracts were incubated with 50 μl magnetic beads conjugated with 4C5 anti-DDK mouse monoclonal antibody (OriGene Technologies) for 2 h at 4°C with gentle agitation. Immune complexes were collected by centrifugation and washed once with lysis buffer and then twice with rinsing buffer (20 mM Tris–HCl, pH 8.0, 2 mM $CaCl_2$). Immunoprecipitated proteins and aliquots of protein extracts were analyzed by immunoblotting using mouse anti-FLAG monoclonal antibody M5 (Sigma-Aldrich) or rabbit anti-human ATF1 monoclonal antibody (Abcam).

Cell viability assays

Adherent cells (typically 2×10^4) were seeded in 48-well plates, cultured for 24 h and then exposed to compound or vehicle. Suspension cells were seeded in 24-well plates at a density of 2×10^5 cells/ml and then exposed to compound or vehicle. To achieve resting conditions, WI-38 cells (10^5 cells in 48-well plates) were cultured for 2 days prior to exposure. Viability of cells was investigated using an alamar blue assay (Biosource). Medium of adherent cultures was removed, and attached cells were incubated in culture medium containing 10% (v/v) alamar blue dye for 4 h at 37°C. To investigate viability of suspension cells, 10% (v/v) alamar blue dye was added directly to the cultures. Medium was collected and, after laser excitation at 530 nm, emitted fluorescence at 590 nm was quantified using a BioTek Synergy4 multimode plate reader (BioTek Instruments). The criterion used to determine necrosis was loss of membrane integrity as measured by the uptake of trypan blue (Sigma-Aldrich). Cells were incubated for 5 min with 0.2% trypan blue and examined by microscopy using a haemocytometer.

Flow cytometry determinations

HeLa cells (3×10^5) were seeded in 6-well plates, cultured for 24 h and then treated with compound 115 or vehicle. MM1.S cells (10^6) were seeded in 60-mm dishes and then treated with compound or vehicle. To determine the percentage of viable cells exposing phosphatidylserine on the outer leaflet of the plasma membrane, cells were harvested and incubated with Annexin V conjugated to Fluorescein isothiocyanate (Annexin V-FITC) and 7-aminoactinomycin D (7-AAD) following the manufacturer´s instructions (Immunostep). Early apoptotic cells were positively stained with Annexin V-FITC but not with 7-AAD. To measure loss of DNA, cells were harvested and fixed in ice-cold 70% ethanol. Fixed cells were collected by centrifugation, incubated for 1 h in PBS containing 50 μg/ml propidium iodide (PI) and 100 μg/ml RNase, and then analyzed by flow cytometry. Cells exhibiting sub-G1 PI incorporation were considered apoptotic. Cells were analyzed by flow cytometry using a FACSCalibur flow analyzer and employing the CellQuest Pro software (BD Biosciences).

Statistical analysis

Unless indicated otherwise, data are presented as means, or means ± SD, of at least three independent experiments. Statistical tests of differential gene expression assessed by microarray analyses and validation by RT-qPCR were performed using the limma software (49). The differences between experimental groups H, C and HT were tested using unpaired *t*-tests and Benjamini–Hochberg method for multiple comparison correction. Other experiments were analyzed using the GraphPad Prism v6 software, using one-way ANOVA followed by Dunnett's multiple comparison test. The criterion for significance in statistical analyses was set at $P \leq 0.05$.

RESULTS

Initial virtual screen to find HSF1 binders

No structure for an entire HSF/HSF1 molecule was known when this study was initiated. However, structural information existed for HSF DNA-binding domains. Eleven structures from yeast (9) and *Drosophila* (2) were available in the Brookhaven Protein Databank. Sequence comparison between *Drosophila* HSF and human HSF1 showed 57% sequence identity and 72% sequence similarity. Using a snapshot from the *Drosophila* NMR structures (1HKT), a

comparative model of the human HSF1 DNA-binding domain was generated. Using this model, four potential cavities were predicted to be large enough to accommodate small drug-like molecules. Based on the potential interactions with residues which line the putative binding pockets, nine three-point pharmacophores were defined and were used to virtually screen a library of 300 000 commercially available lead-like molecules, resulting in the selection and purchase of ∼2000 compounds to constitute a biased sublibrary.

Development of a cell-based assay for human HSF1 DNA-binding domain binders, screen of the biased sublibrary and discovery of compound $I_{HSF}001$

We were interested in any molecule capable of binding the HSF1 DNA-binding domain and affecting the function of the transcription factor, not only in molecules that interfere with DNA-binding (three of the four predicted cavities being distant from the area involved in nucleic acid contact). Consequently, we wished to screen the biased sublibrary employing an assay that reported HSF1-mediated gene expression rather than DNA-binding. Development of a sufficiently discriminating cell-based assay was confounded by the integrated nature of the HSR system. A straightforward assay based on expression of an HSF1-responsive gene likely would have captured many compounds that affect HSF1 activity indirectly such as inhibitors of kinases, activators of phosphatases, enhancers of protein degradation, inhibitors of growth signaling and inhibitors of HSF1 mRNA stability. To exclude such indirectly acting compounds from the screening results to the best extent possible, advantage was taken of the modular nature of HSF1, which permits replacement of the HSF1 DNA-binding domain with an unrelated DNA-binding domain, to create a chimeric transcription factor whose activity is regulated like that of HSF1 but that binds to a different target promoter (43,44). Stable cell line Z74 was developed that was capable of reporting the effects of a compound on the activities of both wild type HSF1 and chimeric HSF1. In order to be considered a true hit, a compound would have to inhibit the activity of wild type HSF1 but not/less chimeric HSF1 (that lacks an HSF1 DNA-binding domain).

Z74 cells contain an inserted gene for chimeric transcription factor LEXA-hHSF1 under the control of a *CMV* early promoter, an *FLUC* gene driven by a promoter responsive to the latter chimeric transcription factor and an *RLUC* gene functionally linked to an *HSP70B* (*HSPA7)* heat shock gene promoter and therefore controlled by endogenous HSF1 (Figure 1A). Both reporter genes are activated by heat shock in a similar dose-dependent fashion (Figure 1B and C). Knockdown by shRNA confirmed that the induced expression of both reporters is dependent on HSF1/chimeric HSF1, although LEXA-hHSF1 appeared to be depleted to a lesser degree than HSF1, and expression of its reporter gene (*FLUC*) to be only effectively reduced under moderately severe stress conditions (Figure 1D). Screening of the sublibrary discovered compound 001 which inhibited RLUC but not FLUC expression in heat-treated Z74 cells (Figure 2A) and which, therefore, appeared to act specifically through the HSF1 DNA-binding domain. (Compound 001 and active derivatives are also referred to herein as HSF1 inhibitors or I_{HSF}.) In a confirmatory experiment, $I_{HSF}001$ was shown to inhibit FLUC expression in a cell line containing an *HSPA7* promoter-driven *FLUC* gene (data not shown).

Analysis of structure–activity relationships

Replacement of the thiazole group present in $I_{HSF}001$ by other five- or six-membered aromatic cycles was examined. Selected results are shown in Table 1A. We found that while some ring substitutions exhibited inhibitory activity in Z74 cells, none showed increased activity over $I_{HSF}001$. Therefore, the thiazole ring was maintained, and effects of substitution at positions R1 and R2 were investigated. Modification at positions R1 and/or R2 often enhanced inhibitory activity, especially when R2 is an aromatic group (Table 1B). Pyridyl addition at R2 increased inhibitory activity most effectively (compound 058; see also Figure 2A). Notable exceptions when R1 was cyclopropyl (compound 053) or carboxylic acid (compound 106) suggest that non-planar or negatively charged groups at this position are detrimental to inhibitory activity. Introduction of a methyl group at the R3 position as in compound 070 significantly enhanced inhibitory activity compared to $I_{HSF}001$ (Table 1C). However, larger groups at R3 resulted in little or no inhibitory activity. Whether the exocyclic C = C double bond was an essential feature to retain activity was also considered. The double bond was modified in two ways. First, it was replaced by the more-flexible C-C single bond to give compound 032 (Table 1D). This compound was devoid of inhibitory activity. Second, structural rigidification of rotatable bonds has been practiced in many systems and has been found to contribute to higher specificity and potency, metabolic stability and improved bioavailability (ref. 50 and references cited therein). The scaffold under investigation was rigidified by replacing the exocyclic C = C double bond with an aromatic bond as in compound 071. The new aromatic ring in compound 071 contains a nitrogen atom 'ortho' to the secondary amine in order to mimic the replaced amide carbonyl oxygen. However, this change also resulted in the loss of inhibitory activity. Substitution at the exocyclic C = C double bond of the scaffold was also investigated. Modification at either R4 or R5 resulted in complete loss of activity as shown by compounds 111 and 085, respectively (Table 1C).

Replacement of the ethyl ester with methyl or isopropyl esters, a ketone or an ether produced inhibitors with reduced potencies (compounds 027, 028, 095 and 097 in Table 1E). Substitution of the ester with an amide also resulted in reduced activity (compound 030). Replacement of the ester with the corresponding acid resulted in inactive compound 004, perhaps owing to the reduced ability of a charged molecule to pass the cell membrane. Out of concern that an ester may not be very stable *in vivo* and may be rapidly hydrolyzed to the inactive acid, we were keen to find a replacement for the ester that would be potentially more stable but retained most of the structural properties of the ester. Compound 001 had been included in the sublibrary as a potential binder of predicted cavity A within the HSF1 DNA-binding domain (defined by Val70, Leu73, Asn74, Phe78, Arg79, Lys80, Thr97, Glu98 and Phe99). Based on

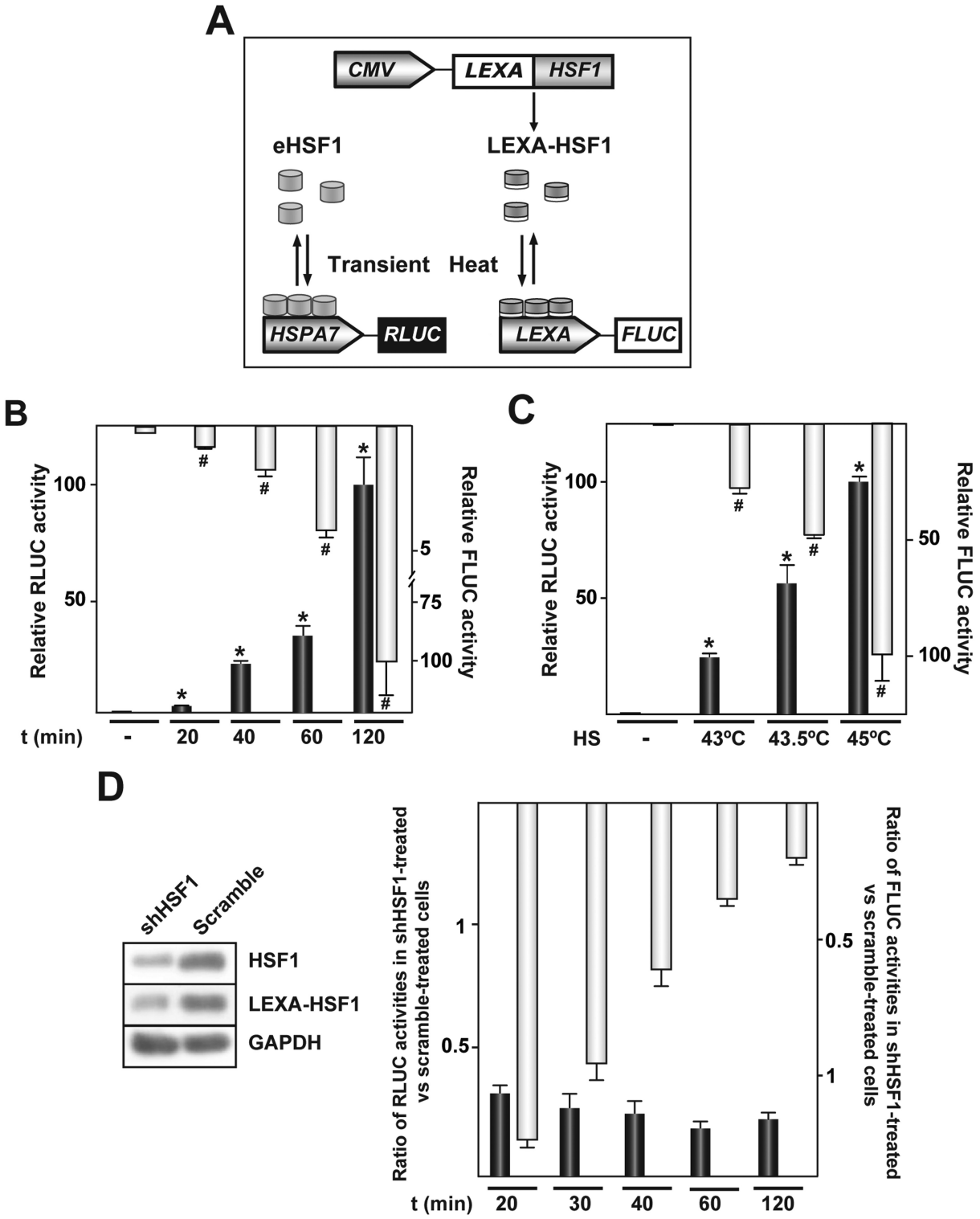

Figure 1. Characterization of Z74 cells. (**A**) Z74 cells harbor an *RLUC* gene that is linked to an *HSPA7* gene promoter. The latter promoter is responsive to endogenous human transcription factor HSF1 (eHSF1). Z74 cells also contain a *CMV* promoter-driven gene for chimeric transcription factor LEXA-HSF1 as well as a *FLUC* gene controlled by a promoter responsive to LEXA-HSF1. Transient heat stimulates the transcriptional activities of eHSF1 and LEXA-HSF1, resulting in increased expression of the *FLUC* and *RLUC* genes. (**B** and **C**) RLUC and FLUC activities in Z74 cells increase as a function of the intensity of their heat exposure. Cells were left untreated (−), were heated (HS) at 42°C for the indicated periods (**B**) or were heated at different temperatures for 30 min (C). RLUC (dark columns) and FLUC (light columns) activities were determined 6 h after heat treatment. $^{*}P < 0.05$; comparing to RLUC activity of untreated cells; $^{\#}P < 0.05$; comparing to FLUC activity of untreated cells. (**D**) Ratios between RLUC and FLUC activities in HSF1 shRNA and control shRNA-expressing cells heated at 43°C for the indicated periods. Levels of HSF1 and LEXA-HSF1 were assessed by WB (on the left).

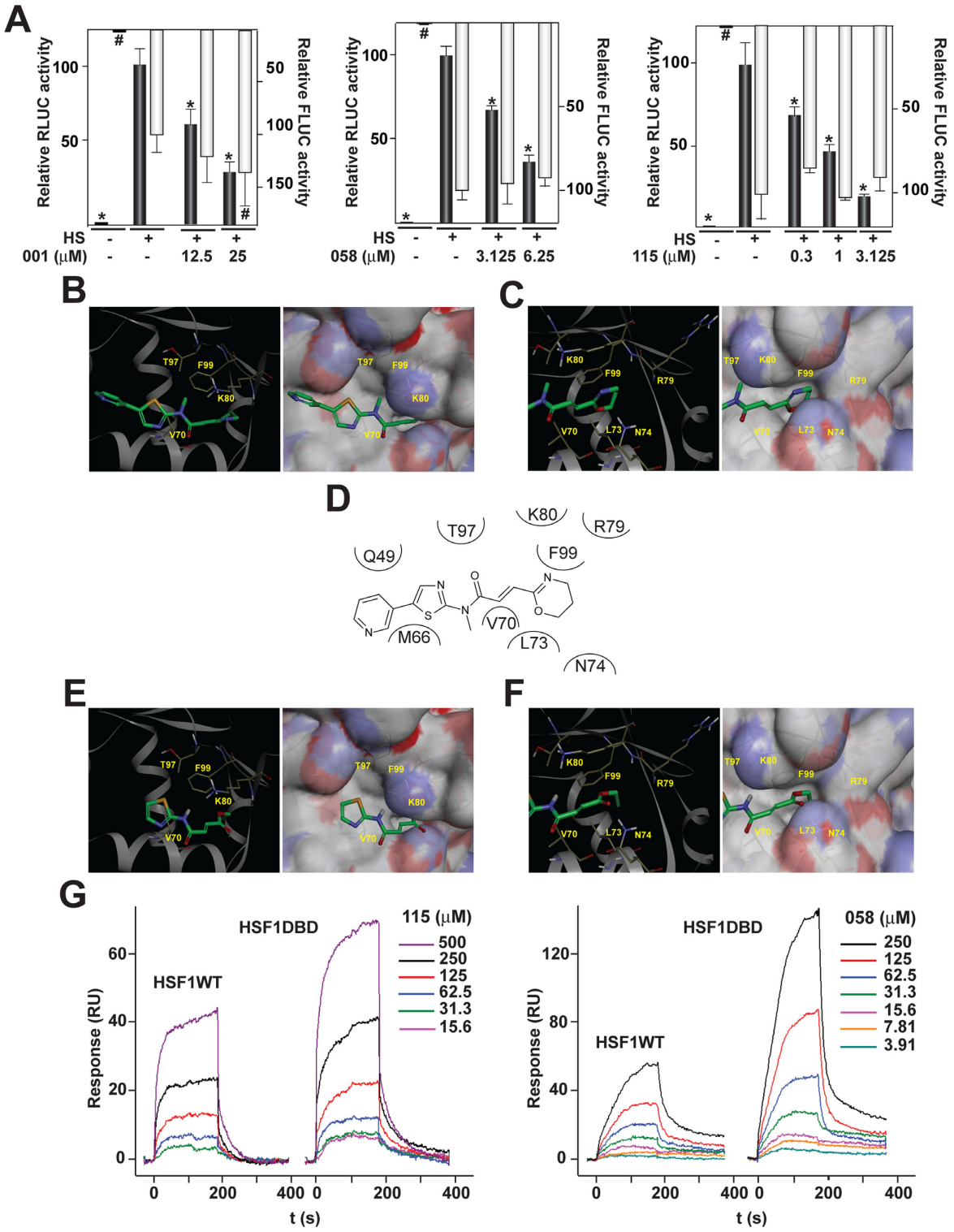

Figure 2. (**A**) Inhibitory activities of $I_{HSF}001$, $I_{HSF}058$ and $I_{HSF}115$ in the Z74 screening assay. Z74 cells, exposed to the inhibitors at the indicated concentrations for 2 h, or exposed to vehicle (−), were heat-treated (HS) at 43°C for 30 min. After 6 h of post-incubation at 37°C (in the continued presence of the inhibitors), RLUC (dark columns) and FLUC (light columns) activities were determined. $^{*,\#}$: $P < 0.05$; comparing to heat-treated cells exposed to vehicle. (**B**–**D**) Docking of $I_{HSF}115$ into predicted cavity A of human HSF1. (B) Images showing the local environment of the R3-methyl in docked $I_{HSF}115$. The residues in close proximity to the methyl group are V70, K80, T97 and F99, which residues partly define the cavity A binding site. The surface shows that there is potentially very limited room for growth at the R3 position. (C) The residues in close proximity to the buried six-membered dihydro-oxazine ring and scaffold double-bond are shown. The surface also reveals that there is limited potential for growth from the double bond. (D) Schematic representation of residues in close proximity to $I_{HSF}115$. (**E** and **F**) Docking of $I_{HSF}001$ into predicted cavity A of human HSF1 (E). Images showing the local environment of the R3-unsubstituted amide NH in docked $I_{HSF}001$. (F) Residues in close proximity to the ethyl ester group and scaffold double-bond. (**G**) SPR sensorgrams documenting interactions between $I_{HSF}115$ or $I_{HSF}058$ and (His-tagged) recombinant HSF1WT or HSF1DBD proteins.

Table 1. Structure–activity relationships

A

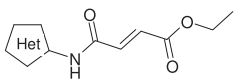

Cpd	het	IC_{50} (μM)
001		**17.8 +/-** 2.6
015		>25
018		23.6
019		ND
020		23.5
023		ND
044		>25

B

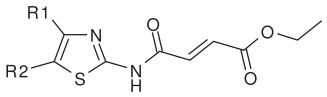

Cpd	R1	R2	IC_{50} (μM)
011	Me	H	7.0
012	Ph	H	11.3
053	c-Propyl	H	>25
054	2-Py	H	20.2
055	3-Py	H	18.7
056	4-Py	H	19.8
013	H	Me	25.0
014	H	Ph	7.1
058	**H**	**3-Py**	**4.8 +/-** 0.4
059	H	2- Me-Ph	14.7
051	Me	Ph	9.6
052	Me	Me	7.4
105	COO-Me	Ph	10.8
106	COO^-	Ph	ND
107	Et	Ph	10.6
109	CONH2	Ph	11.2

C

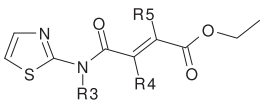

Cpd	R3	R4	R5	IC_{50} (μM)
070	**Me**	**H**	**H**	**5.7** +/- 0.8
100		H	H	ND
101	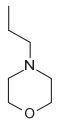	H	H	>25
085	H	H	Me	ND
111	H	Me	H	ND

D

Cpd	R6	IC_{50} (μM)
032	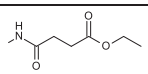	ND
071	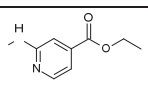	ND

E

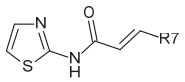

Cpd	R7	IC_{50} (μM)
004		ND
027		>25
028		>25
030		>25
095		>25
097		ND
087		ND
088		>25
089		17.9
090		**5.4 +/-** 0.4

F

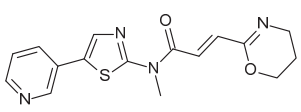

Cpd. 115 IC_{50} (μM) : 0.7 +/- 0.1

IC_{50} values represent concentrations of compounds required for 50% inhibition of heat-induced RLUC activity in Z74 cells. IC_{50} values were estimated by extrapolation from two data points exhibiting >50% inhibition and <50% inhibition, respectively. Representative values are shown. For several key compounds, IC_{50} values were determined from full activity/concentration curves, and SD values were estimated. ND: no activity detected.

the hypothesis that compound 001 in fact binds in the latter cavity, a docking experiment was carried out that compared compound 001 with virtual compounds in which the ester had been replaced with five- or six-membered rings. Results suggested that rings of the latter size could be accommodated by the cavity (see the docking experiment discussed below). A set of compounds with different ester replacements was synthesized and tested for inhibitory activity. Whereas most replacements resulted in compounds with lower inhibitory activity than compound 001, a partially unsaturated heterocycle produced a compound with considerably better inhibitory activity (compound 090).

Finally, we combined those individual modifications that had most effectively improved inhibitory activity. These modifications included addition of a 3-Py at position R2, a methyl group at R3 and substitution of the carboxylate ester with the partially unsatured dihydro-oxazine heterocycle of compound 090. The resulting compound, $I_{HSF}115$, was clearly a better inhibitor in Z74 cells than lead compound 001 or the compounds containing the individual modifications (Table 1F). $I_{HSF}115$ had substantial activity in the high nanomolar/low micromolar range (see also Figure 2A).

A docking study was conducted to identify potential binding modes of $I_{HSF}115$ and rationalize the observed improvement in activity. The docking program 'GOLD' (51) was employed for docking $I_{HSF}115$ into cavity A. Up to 5000 docking solutions were allowed, in which each docking had to deviate from the previously generated solutions by a minimum of 2.0Å RMSD with respect to heavy atoms. This approach allowed the exhaustive exploration of the potential binding modes of $I_{HSF}115$ in cavity A. The resulting dockings were then analyzed; a valid pose needed to (i) place the R3 substituent into a position where very small alkyl groups are tolerated but larger groups would clash with the binding site, (ii) place both R4 and R5 positions of the scaffold in such a way as to not accommodate any potential substituents at these positions and (iii) place the partially unsaturated six-membered heterocycle into a small pocket, thus not tolerating significant growth of the group. Docking of molecule 115 into cavity A yielded an interesting binding mode, which largely agreed with the structure–activity results (Figure 2B–D). The docking mode has the following notable features: the N-Me group is buried into a well-defined hydrophobic sub-pocket defined mostly by the side-chains of Val70, Lys80, Thr97 and Phe99. The bulky sulfur atom in the thiazole ring also points toward this pocket. The partially unsaturated six-membered heterocycle (5,6-dihydro-4H-1,3-oxazine) is accommodated into another sub-pocket, but appears to make no formal hydrogen bonds with the homology model. However, the group could potentially interact with the side chain of Asn74 and, further away (about 5.0Å), the side chain of His83 through a water-mediated interaction. For the sake of completeness, an analogous docking experiment conducted with $I_{HSF}001$ is reported in Figure 2E and F.

Further investigation focused on best inhibitor $I_{HSF}115$. However, several experiments also included $I_{HSF}058$ as an example of compounds that displayed properties not seen with $I_{HSF}115$.

SPR was used to confirm that the inhibitors of human HSF1 function interact directly with the transcription factor and, more specifically, its DNA-binding domain. Recombinant human HSF1 or a recombinant DNA-binding domain fragment of human HSF1 served as ligands. As revealed by the SPR sensorgrams in Figure 2G, both compounds tested, i.e. $I_{HSF}058$ and $I_{HSF}115$, interacted in a dose-dependent fashion with both full-length HSF1 (HSF1WT) and the HSF1 DNA-binding domain (HSF1DBD) fragment. These results provide strong evidence that the compounds directly bind the HSF1 DNA-binding domain. It is noted that evidence for interaction was obtained at compound concentrations (15.6 μM and higher) that were above those that cause inhibition of induced RLUC expression in Z74 cells. This difference in sensitivity may be due to conformational constraints imposed by the method of immobilization of the polypeptides on the sensor chips (amine coupling). Alternatively, or in addition, the recombinant HSF1WT and HSF1DBD fragments that lack all critical modifications of HSF1 as well as its normal cover of chaperones and other cofactors may not have been able to acquire a quasi-native and fully competent conformation.

Mode of action of HSF1 inhibitors

In a first set of experiments, cultures of Z74 cells were exposed to different concentrations of $I_{HSF}058$ or $I_{HSF}115$, heat-treated and post-incubated for 1 h. Total RNA was isolated, and poly-adenylated RNA quantified by RT-qPCR. Exposure of the cells to the compounds resulted in a dose dependent reduction of transcript levels of the *HSPA7* promoter-driven *RLUC* gene (Figure 3A, left graph). $I_{HSF}115$ was somewhat more effective than $I_{HSF}058$ in inhibiting accumulation of transcripts. It is noted that substantial effects already occurred at 1 μM concentrations. Similar results were obtained when total *RLUC* RNA was quantified (Figure 3A, right graph). We take these data to reflect effects of the inhibitors on HSF1-mediated *HSP* promoter-driven gene transcription. Although we have not investigated effects at the level of transcript stability, the fact that the compounds were designed to bind to HSF1 and were shown to do so renders this possibility somewhat remote. Analogous dose-dependent inhibitory effects on transcript accumulation were observed for the endogenous *HSPA1A* and *HSPA7* genes, although larger compound concentrations were needed to achieve comparable inhibition effects to those seen for the *RLUC* gene, possibly owing to some compensatory mechanism(s) (Figure 3B and C). Heat-induced accumulation of inducible HSP72 (mainly products of the *HSPA1A* and *HSPA1B* genes) was assessed by WB (Figure 3D). Inhibitory effects of $I_{HSF}115$ were observable at 3.125 μM and were substantial at 6.25 μM. $I_{HSF}058$ was less effective than I_{HSF} 115.

To examine whether the inhibitors affected sequence-specific DNA-binding of HSF1, extracts were prepared from HeLa cells that had been exposed for 2 h at 37°C to different concentrations of $I_{HSF}058$, $I_{HSF}115$ or vehicle and then heat-treated for 30 min at 43°C. Electrophoretic mobility shift assay (EMSA) using an HSE oligonucleotide probe showed that $I_{HSF}058$, but not $I_{HSF}115$, prompted a dose-dependent reduction of DNA-binding activity (Figure 4A, top). An anti-HSF1 WB revealed a dose-dependent

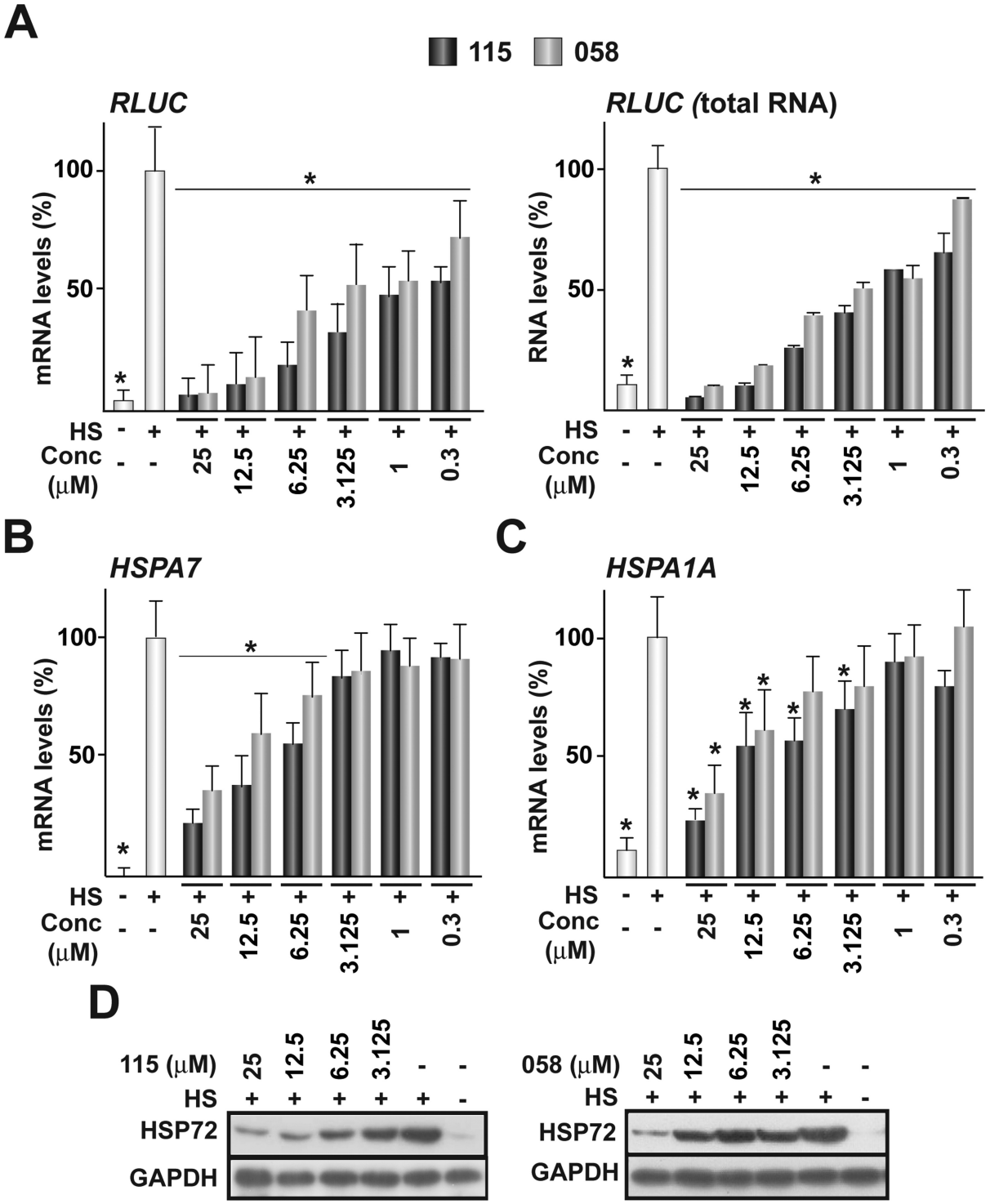

Figure 3. (**A**–**C**) Inhibitory activities of $I_{HSF}058$ and $I_{HSF}115$ assessed at the transcript level by RT-qPCR. Z74 cells, exposed to the inhibitors at the indicated concentrations for 2 h, or exposed to vehicle (−), were heat-treated (HS) at 43°C for 30 min and post-incubated at 37°C for 1 h (in the continued presence of inhibitors). (A) Relative *RLUC* mRNA (left graph) and *RLUC* total RNA (right graph) levels. (B) Relative *HSPA7* mRNA levels. (C) Relative *HSPA1A* mRNA levels. $*P < 0.05$; comparing to heat-treated cells exposed to vehicle. (**D**) Inhibition of HSP72 expression assessed by WB. Z74 cells were treated as under (A–C), except that post-incubation at 37°C was for 6 h.

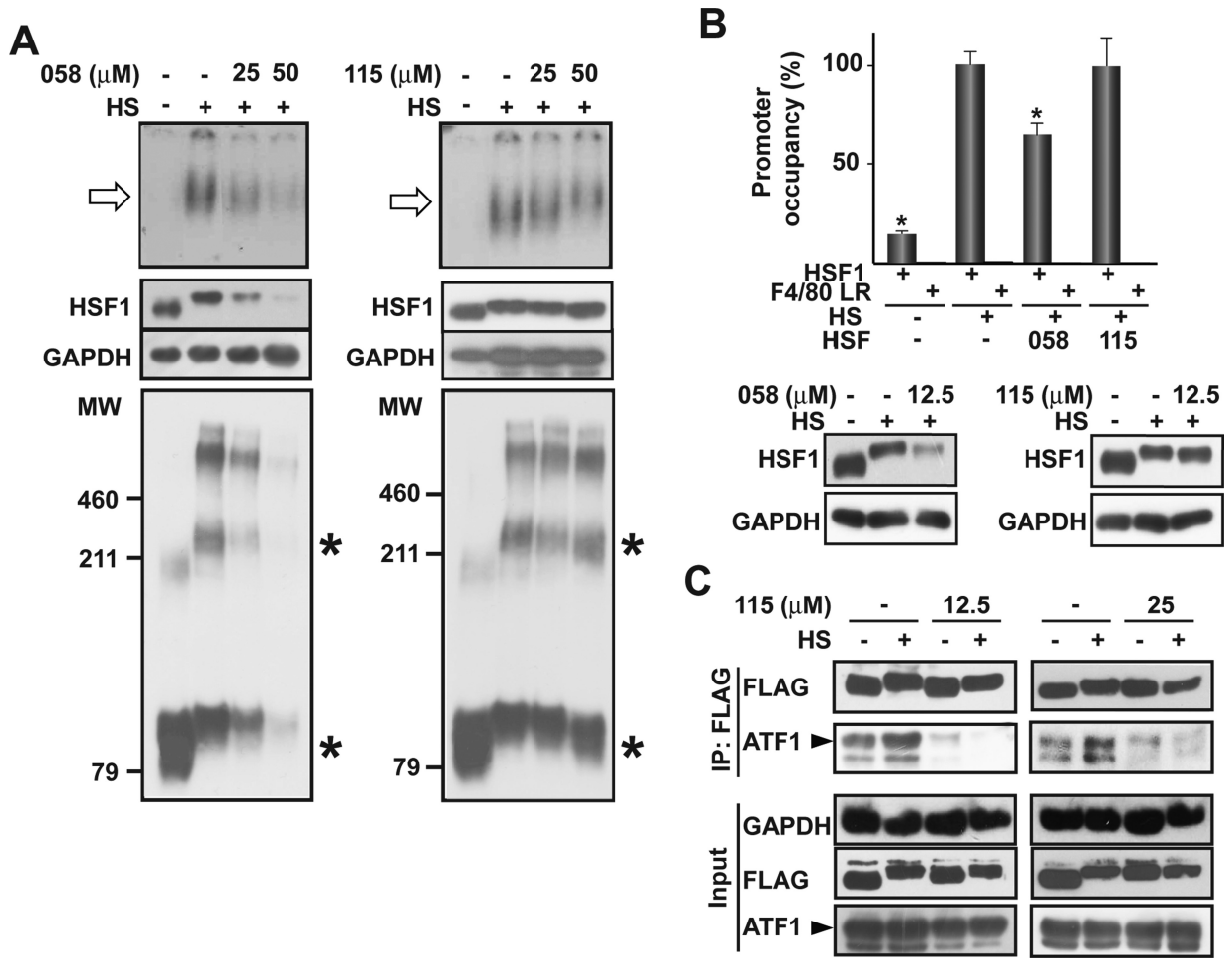

Figure 4. On the mechanism of action of I_{HSF}. (**A**) Effects on HSF1 DNA-binding ability, stability and oligomerization. Analyzed were extracts from HeLa cells that were vehicle-treated or pre-treated for 2 h with the indicated concentrations of $I_{HSF}058$ or $I_{HSF}115$ and then exposed to 43°C heat for 30 min (HS). Top: HSF1 DNA-binding ability determined by EMSA. The arrows indicate the positions of the major HSF1–HSE probe complexes. Middle: HSF1 immunoblot. GAPDH served as loading control. Bottom: HSF1 immunoblot after EGS cross-linking of HSF1 in oligomers. The positions of pre-stained molecular weight marker proteins (MW, in thousands) are indicated to the left. Asterisks indicate the positions of monomeric and trimeric HSF1. (**B**) Top: effects on the recruitment of HSF1 to the *HSPA1A* promoter. HeLa cells, exposed to $I_{HSF}058$ or $I_{HSF}115$ at 12.5 μM, or exposed to vehicle (−), were heat-treated (HS) at 43°C for 30 min and then processed for ChIP using anti-HSF1 or anti-F4/80 LR (control) antibodies. $*P < 0.05$; comparing to heat-treated cells exposed to vehicle. Bottom: anti-HSF1 WB of extracts from cells exposed to identical conditions. (**C**) Co-immunoprecipitation of ATF1. Left and right halves show results from independent experiments. CTF135 cells expressing a C-terminally FLAG-tagged HSF1 were vehicle-treated (−) or pre-treated with 12.5 or 25 μM $I_{HSF}115$, heat-treated (HS) at 43°C for 30 min and then processed for immunoprecipitation with an anti-FLAG antibody. Immunoprecipitates (IP:FLAG) and aliquots of extracts (input) were analyzed by anti-FLAG and anti-ATF1 immunoblot.

destabilization of HSF1 by compound 058 (Figure 4A, middle). It appeared that this effect can account for the reduced HSE DNA binding observed with extracts from $I_{HSF}058$-exposed cells. The most potent inhibitor, $I_{HSF}115$, did not display this property. That $I_{HSF}115$ (and $I_{HSF}058$ apparently as well) did not inhibit HSF1 DNA-binding activity implied that heat-induced homo-oligomerization of HSF1 was also not affected by the compounds. To verify this, aliquots of the same extracts that were tested in the above EMSA assays were exposed to EGS to cross-link HSF1 oligomers and re-analyzed by anti-HSF1 WB. No impairment of HSF1 oligomerization by $I_{HSF}115$ or $I_{HSF}058$ could be observed (Figure 4A, bottom). To find out whether the compounds reduced HSF1 DNA binding in the chromatin context, we carried out ChIP experiments on similarly treated HeLa cells (at compound concentrations of 12.5 μM). Cultures were processed as described in 'Materials and Methods' section. DNA fragments precipitated by HSF1 antibodies were amplified by qPCR using primers that delineate a promoter segment of the *HSPA1A* gene including the proximal HSE sequence (HSF1 target sequence) and the TATA box sequence. $I_{HSF}115$ was found not to cause any reduction in HSF1 binding (Figure 4B, top). However, significantly decreased promoter occupancy was observed in $I_{HSF}058$-treated cells. Again, this decrease could be readily explained as an effect of destabilization of HSF1 by the compound as evidenced by an anti-HSF1 WB of extracts from cells exposed to identical conditions (Figure 4B, bottom). It is noted that the absence of an effect of $I_{HSF}115$ on promoter occupancy also implies that the compound does not interfere with nuclear import of HSF1 in a significant fashion.

By way of elimination, the above analysis suggests that HSF1 inhibitors (at least those of the $I_{HSF}115$ type) affect the transactivation function of HSF1. It is known that ATF1/CREB regulates the stress-induced HSF1 transcription complex and mediates the recruitment of mammalian HSF1 to its target promoters (19). ATF1/CREB interacts with the HSF1 DNA-binding domain. We investigated whether $I_{HSF}115$ was capable of interfering with the HSF1–ATF1 interaction. Use was made of a HeLa-derived cell line that stably expresses a C-terminally FLAG-tagged HSF1. Cultures were heat-treated for 30 min at 43°C in the presence or absence of $I_{HSF}115$, extracts were prepared and tagged HSF1 was immunoprecipitated using an anti-FLAG antibody. WB analysis of immunoprecipitates revealed that $I_{HSF}115$ dramatically reduced the HSF1–ATF1 interaction (Figure 4C). Based on this finding, we suggest that $I_{HSF}115$ interferes with the formation of ATF1-based transcription complexes that is instrumental in heat-induced transcription of HSF1 target genes.

Using inhibitor $I_{HSF}115$ to probe the human heat shock response (HSR) at the transcript level

HeLa cells were either subjected to a heat treatment at 43°C/30 min and then post-incubated at 37°C for 1 h or were maintained at 37°C. The latter relatively mild heat shock conditions (employed also in most other experiments of the present study) were chosen to avoid stress-induced perturbations to the best extent possible. Exposure to $I_{HSF}115$ began 2 h before heat treatment. RNA was isolated and analyzed by hybridization to Affymetrix microarrays. It is noted that WB analysis of similarly treated cells revealed that HSF1 was not destabilized by $I_{HSF}115$ (Figure 5A, lower two blots). We restricted our analysis to protein-coding genes (except for *HSPA7*) whose transcript levels changed by at least 1.4-fold (in either direction) after heat treatment. This resulted in sets of 667 heat-induced and 406 heat-repressed genes (column H/C in Supplementary Table S2, Supporting Information; H: heat-treated; C: control-treated). For comparison purposes (see below), the numbers given are for the 511 most highly heat-induced genes. The heat-induced increases in transcript levels of many of these genes were inhibited partially to completely by $I_{HSF}115$ (HT/H ratios significantly lower than 1, and (HT-C)/(H-C) ratios lower than 1; see Supplementary Table S2; HT: heat-treated and I_{HSF}-exposed). Based on the latter findings of inhibition, 328 heat-induced genes (64.2%) were classified as positively regulated by HSF1. Values significantly lower than 1 in column HT/C (and negative (HT-C)/(H-C) values) were observed for 19 of these genes, suggesting that their expression in HeLa cells was supported by HSF1 even in the absence of a stress. The transcript levels of seven genes (1.4%) had risen in heat-treated cells in the presence of $I_{HSF}115$ (HT/H ratios significantly higher than 1, and (HT-C)/(H-C) ratios higher than 1). These heat-induced genes appeared to be negatively regulated by HSF1. Finally, 176 heat-induced genes (34.4%) were considered not-regulated by HSF1 (HT/H ratios not significantly different from 1). Results obtained for the 50 most highly heat-induced genes are visualized in Figure 5B (columns 'HeLa'). The fraction of genes that are positively regulated by HSF1 may be considerably higher than is suggested by the above estimate of 64.2% and may reach a figure as high as about 80%. Percentages of $I_{HSF}115$-inhibited genes within groups of 100 heat-induced genes with decreasing heat inducibility (H/C ratios equal to or greater than 2.822, 2.022, 1.733, 1.610, 1.505, 1.432 and 1.401 for the remainder group of 67 genes) were found to decrease essentially monotonously from 75 to 43% (Figure 5C, top left). The best explanation for this unusual correlation appears to be that, with decreasing heat induction, partial inhibition by $I_{HSF}115$ increasingly fails to reach statistical significance. Thus, in groups with increasingly smaller heat inducibility, the number of HSF1-regulated genes that fail to be recognized and, consequently, apparent average efficacy of I_{HSF} inhibition increase (see Figure 5C, top right). Corresponding data for cell line HF73 (see below) are presented in Figure 5C, bottom graph.

A very different picture emerged for the heat-repressed genes (see Figure 5E, columns 'HeLa', for a visualization of effects seen for the 50 most highly heat-repressed genes). Most of these genes (292, representing 71.9% of repressed genes) were classified as not regulated by HSF1 (HT/H ratios not significantly different from 1). Perhaps, these genes are subject to a global repression mechanism(s). Nevertheless, $I_{HSF}115$ caused partial to near complete relief from repression in 87 (21.4%) of the heat-repressed genes (HT/H ratios significantly higher than 1, and (HT-C)/(H-C) ratios lower than 1; Supplementary Table S2). These genes are considered negatively regulated by HSF1. That exposure of cells to $I_{HSF}115$ essentially reverses the repressive effect of heat treatment on the expression of certain genes strongly suggests that the inhibitor does not exert a generalized inhibitory effect on transcription. As a corroboration, exposure of HeLa cells transfected with constitutively expressed luciferase genes to $I_{HSF}115$ for 6 h had only a marginal effect on reporter gene expression (not shown). A small number of heat-repressed genes (27 (6.7%)) appeared to be positively HSF1-regulated.

An earlier genome-wide gene expression microarray study in HeLa cells had reported 511 heat-induced and 1305 heat-repressed genes (29). HSF1-regulated genes were identified by comparing heat regulation in HSF1-depleted and not-depleted cells. The findings of the latter study are summarized in Table 2. In the present study, HSF1 regulation was revealed by positive or negative effects of $I_{HSF}115$ on gene transcription. To compare our data with those of the earlier study, we added in Table 2 information on the 511 most highly heat-induced genes and all heat-repressed genes of the present study. The results of the two studies are surprisingly different. The earlier study identified 137 genes that were positively regulated by HSF1 (26.8%). Similar frequencies were reported in a recent study in mouse embryo fibroblasts (52). Our study suggests that the heat induction of at least 328 of the 511 genes (64.2%) was mediated by HSF1. Thus, 2.4-times as many positively HSF1-regulated genes were identified based on the immediate effects of a specific HSF1 inhibitor than based on the delayed effects of HSF1 depletion. Among the heat-repressed genes, similar estimates of the fraction of HSF1-repressed genes were obtained from inhibition of HSF1 transcriptional activity (21.4%) and HSF1 depletion (20.8%). Numbers of genes with complex regulation were substantially smaller when

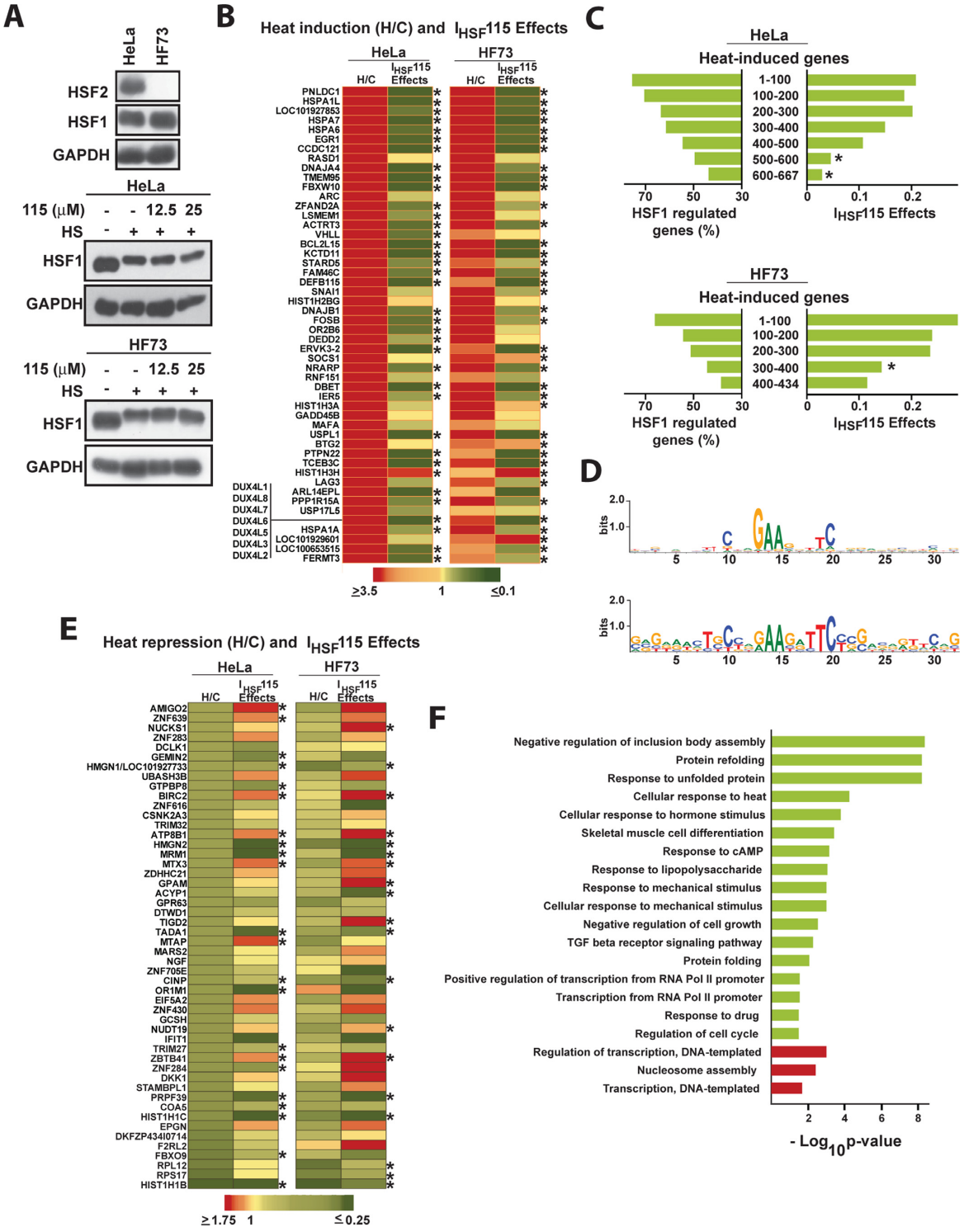

Figure 5. Transcriptome analyses. (**A**) Top: WB showing expression of HSF1 and HSF2 in HeLa and HF73 cells, respectively. Lower blots: HeLa or HF73 cells were vehicle-treated or exposed to 12.5 or 25 μM $I_{HSF}115$ for 2 h, heat-heated at 43°C for 30 min and post-incubated at 37°C for 1 h or vehicle-treated and incubated at 37°C for 3.5 h. Extracts were analyzed for HSF1 levels. (**B** and **E**) HeLa and HF73 cells were similarly treated (at 25 μM $I_{HSF}115$), and RNA was extracted and analyzed using Affymetrix microarrays. HT: heat-treated and $I_{HSF}115$-exposed; H: heat-treated; C: vehicle-treated. (B) Heatmaps showing heat inducibility (H/C) in the left columns and effects of $I_{HSF}115$ on heat-induced expression ($I_{HSF}115$ effects: (HT-C)/(H-C)) in the right columns for the 50 most highly heat-induced genes in HeLa cells. *$P < 0.05$ between HT and H. (**C**) Left: fractions of HSF1-regulated genes in groups of 100 heat-induced genes. Right: $I_{HSF}115$ Effects ((HT-C)/(H-C)). See the 'Results' section for further explanations. *$P < 0.05$; comparing to group 1–100. (**D**) HSE sequences. Top: consensus (gene-proximal) HSE derived from a group of 30 heat-induced, HSF1-regulated genes. Bottom: consensus HSE derived from a group of classical heat shock genes. The logograms were generated at http://weblogo.berkeley.edu. (E) Heatmaps as in (B), but for the 50 most highly heat-repressed genes in HeLa cells. (**F**) GO analyses (biological processes). Light green: heat-induced, positively HSF1-regulated genes; red: heat-repressed, negatively HSF1-regulated genes.

estimated from effects of $I_{HSF}115$ instead of from differences in gene expression between HSF1-depleted and control cells. This concerns heat-induced genes whose activity is limited by active HSF1 (1.4 versus 7.4%), and heat-repressed genes whose activity appears to be positively affected by active HSF1 (6.7 versus 17.7%).

HeLa cells express HSF2, another member of the HSF family. HSF2 is known to bind to HSE sequences in the promoters of many heat-regulated genes as well as to form heterooligomeric complexes with HSF1 (53,54). While apparently not able to function as a transcription factor on its own, HSF2 was found to enhance/reduce HSF1-mediated expression of major *HSP* genes (55,56). To find out whether HSF2 modulates I_{HSF} effects or may even be required for these effects, we used CRISPR technology to obtain a HeLa-derived cell line deficient for HSF2 and repeated the microarray analysis (Figure 5A, top blot). We found 434 heat-induced and 220 heat-repressed protein-coding genes in HSF2-deficient line HF73 (column H/C in Supplementary Table S3, Supporting Information). Of the 511 most highly heat-induced genes in HeLa cells, 407 were less highly heat-induced in HF73 cells, 26 were more highly heat-induced and 78 were unchanged (<10% change in the H/C ratio) (see Supplementary Table S4, Supporting Information). This finding is consistent with the notion that HSF2 is an important cofactor of HSF1 that generally affects heat-induced gene expression. Based on their transcriptional responses to $I_{HSF}115$, 267 of the 434 heat-induced genes of HF73 cells (61.5%) were considered to be regulated by HSF1 (Table 2; see also Figure 5B and E, columns 'HF73'). This frequency is similar as that observed in HeLa cells, where 335 of 511 heat-regulated genes (65.6%) were HSF1-regulated. Clearly, I_{HSF} function is not dependent on HSF2. Closer inspection of results revealed remarkable qualitative changes in the regulation of heat-induced genes that may have been caused by the absence of HSF2. Twenty-one heat-induced genes that were positively HSF1-regulated (3) or unregulated (18) in HeLa cells showed as negatively HSF1-regulated in HF73 cells (Supplementary Table S4). Moreover, 50 genes that were positively regulated in HeLa cells were found unregulated by HSF1 and 15 genes that had been unregulated in HeLa cells positively HSF1-regulated in HF73 cells. Among the 220 heat-repressed genes identified in HF73 cells, 97 (44.1%) appeared to be HSF1-regulated (Table 2). The fractions of both negatively and positively regulated heat-repressed genes were increased in HF73 cells compared with HeLa cells.

HSF1 acts through HSE sequences in the promoters of the genes it controls. The ability to identify HSF1-regulated genes by their susceptibility to an HSF1 transcriptional inhibitor provided us with an opportunity to define an HSE consensus sequence based on a functional criterion. Such a sequence derived from a group of 30 $I_{HSF}115$-inhibited genes exhibiting different levels of heat inducibility is shown in Figure 5D (top logogram). It contains two complete NGAAN modules of which one is less prominent than the other. An HSE consensus sequence obtained from a group of classical heat shock genes looks notably different, featuring four or five modules, of which three are similarly prominent (bottom logogram). The latter sequence resembles a consensus sequence that had been derived from an analysis of *in vivo* binding sites of HSF1 (30). It therefore appears that somewhat degenerate HSE sequences remain capable of conferring heat regulation on an associated gene, even though binding of HSF1 to such elements may not be detected by currently used methods. The above group of 30 example genes was also searched for transcription factor binding sites known to be associated with heat-regulated genes (52). Binding sites for AP1, SRF, YY2 and ELF1 were each present in about 60% of the genes. The average distance of these elements from the transcription start site was generally similar as that of the promoter-proximal HSE sequence.

The present study classified a far greater proportion of heat-induced genes as positively HSF1-regulated genes than the most relevant previous study (29). To find out whether we could discover additional gene categories that had not been associated previously with regulation by HSF1, we carried out a GO analysis using the David bioinformatics resources (48). The range of biological processes that involve positively HSF1-regulated genes uncovered by this analysis is represented in Figure 5F. Categories identified include proteotoxic stress-related categories such as 'protein refolding', 'response to unfolded proteins', 'cellular response to heat' and 'protein folding'. However, they also include categories such as 'response to hormone stimulus', 'skeletal muscle differentiation', 'response to cAMP', 'response to lipopolysaccharide', 'response to mechanical stimulus', 'negative regulation of cell growth', 'regulation of transcription from Pol II promoters' (positive and negative) and 'regulation of cell cycle'. Prominent categories of negatively HSF1-regulated genes are 'regulation of transcription' and 'nucleosome assembly'. The complete results of this analysis are shown in Supplementary Table S5, Supporting Information.

I_{HSF} impair the viability of cancer cells

Cancer cells are dependent on HSF1 for growth as has been demonstrated by siRNA knockdown (31). Compounds that inhibit HSF1 function are expected to have analogous effects on cancer cells. We assessed the viability of HeLa cells exposed for 96 h to different concentrations of $I_{HSF}001$, 058 and 115 using an alamar blue assay (Figure 6A). Viability decreased in a dose-dependent fashion with $I_{HSF}115$ being considerably more effective than $I_{HSF}058$ and 001. The relative cytotoxicity of the compounds is approximately in line with their respective strengths as inhibitors of HSF1 activity. Subsequently, we explored effects of $I_{HSF}115$ on viability in a panel of different human cancer cell lines (Figure 6B). HSF1 has been described as being required for optimal p21 expression and p53-mediated cell cycle arrest in response to genotoxins, suggesting that the factor may also play a p53-dependent pro-apoptotic function (57). To test whether responsiveness to $I_{HSF}115$ depended on p53, cell lines of different p53 status were included in the panel. Results showed that all cell lines suffered a loss in viability upon exposure to $I_{HSF}115$, although sensitivity varied widely. No systematic effect of loss of p53 function could be detected. HSF1 is the master regulator of inducible HSP expression, and HSPs are key components of the cell's mechanism for proteostasis maintenance. That levels of activated

Table 2. Heat regulation by HSF1—results obtained based on HSF1 depletion or HSF1 inhibition

Regulation by HSF1	RNA levels after heat treatment					
	Increased			Decreased		
Cell type	HeLa	HeLa	HF73*	HeLa	HeLa	HF73
No regulation	336 (65.8%)	176 (34.4%)	167 (38.5%)	802 (61.5%)	292 (71.9%)	123 (55.9%)
Negative regulation	38 (7.4%)	7 (1.4%)	39 (9.0%)	272 (20.8%)	87 (21.4%)	65 (29.6%)
Positive regulation	137 (26.8%)	328 (64.2%)	228 (52.5%)	231 (17.7%)	27 (6.7%)	32 (14.5%)
	HSF1 siRNA depletion**	$I_{HSF}115$ inhibition (present study)		HSF1 siRNA depletion**	$I_{HSF}115$ inhibition (present study)	

*HSF2-deficient HeLa-derived line.
**The depletion data are from ref. 29.

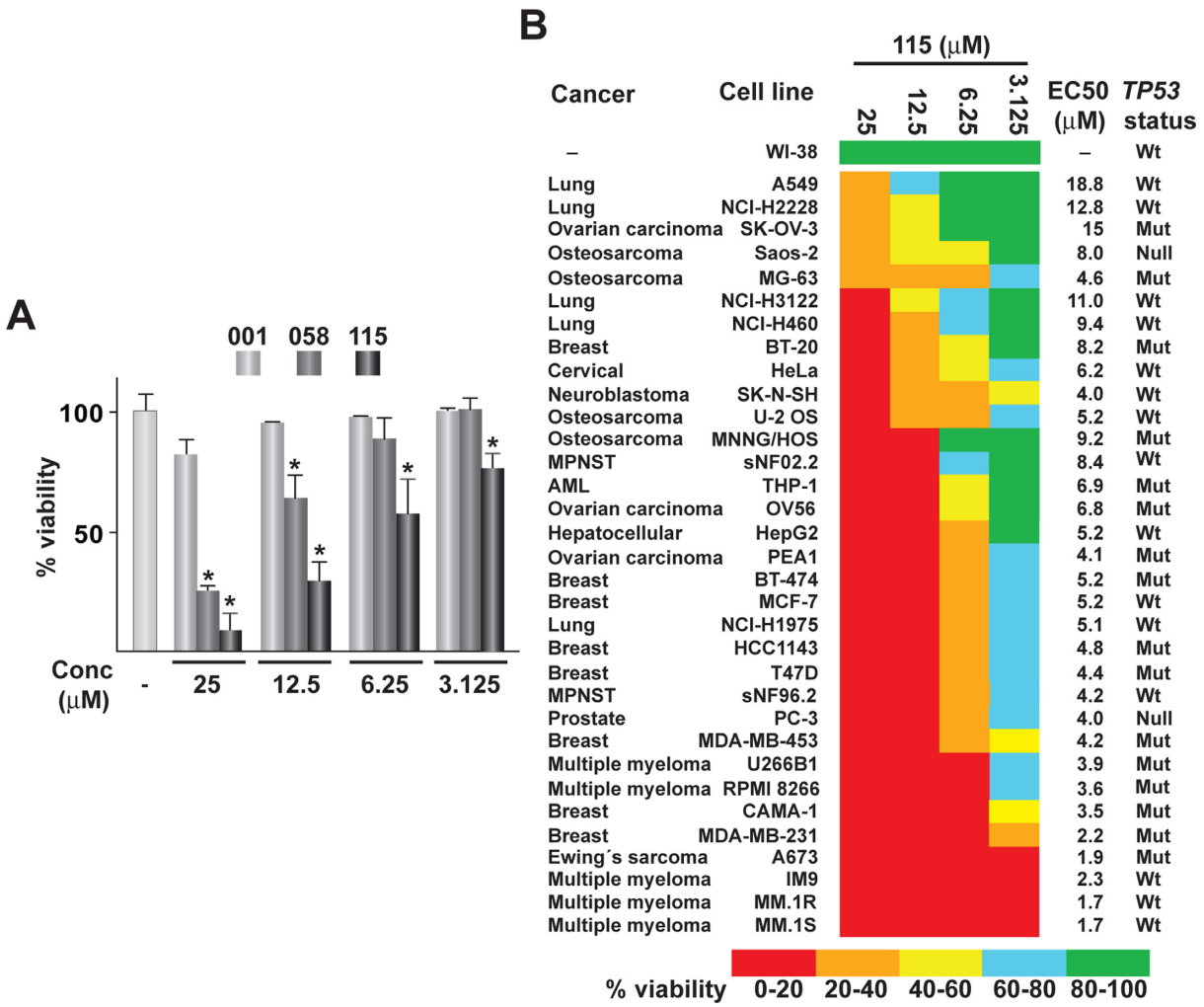

Figure 6. (**A**) Viability of HeLa cells that had been exposed for 96 h to the indicated concentrations of $I_{HSF}001$, $I_{HSF}058$ or $I_{HSF}115$, or to vehicle (−). *$P < 0.05$; comparing to cells exposed to vehicle. (**B**) Heatmap summarizing viability data obtained for different cell lines. AML: acute myeloid leukemia. MPNST: malignant peripheral nerve sheath tumor. Wt: wild-type. Mut: mutated. EC50: dose causing a 50% reduction in viability.

HSF1 tend to be elevated in cancer cells suggests that these cells may require elevated levels of HSPs for coping with an increased load of mutated proteins with non-native conformations (30,38). An increased requirement for chaperones may be readily rationalized for cells whose growth is driven by proteins expected to be conformationally compromised such as fusion kinases or mutation-activated kinases. Results showed that EML4-ALK fusion kinase-expressing cell lines NCI-H3122 and NCI-H2228 or mutation-activated EGFR kinase-expressing line NCI-H1975 are not especially responsive to $I_{HSF}115$. Proteostasis maintenance appears to be particularly challenged in multiple myeloma cells that are highly sensitive to inhibition of proteasome function (58). We found that multiple myeloma lines consistently exhibited moderately high to high sensitivity to $I_{HSF}115$. It is noted that the inhibitor was also highly cytotoxic in two

breast cancer lines (CAMA-1, MDA-MB-231) and an Ewing sarcoma line (A673).

Mode of I_{HSF}115-induced cell death

To ascertain that cancer cells were in fact killed by I_{HSF}115, parallel sets of HeLa and MM.1S cell cultures were exposed for 6, 15, 24 or 96 h to increasing concentrations of the compound. Cells were stained with Trypan Blue, and stained (necrotic) and unstained (live) cells were counted. Figure 7A shows numbers of live cells, and Figure 7B percentages of dead cells. Exposure to I_{HSF}115 reduced the number of live cells and increased the number of necrotic cells in both concentration- and time-dependent fashions. Whereas cell killing trumped proliferation of MM.1S cells already at a 3.125 μM concentration of I_{HSF}115, much higher concentrations were needed for HeLa cells. At 12.5 or 25 μM concentrations of I_{HSF}115, most MM.1S cells were killed after 6 h of exposure. Longer exposures were required to achieve comparable effects in HeLa cells.

To investigate whether apoptosis was a major mechanism of death after treatment with I_{HSF}115, cells exposed to the compound for 6 h were double-stained with Annexin V-FITC and 7-AAD. Live apoptotic cells (Annexin V^+/7-AAD^-) are expressed as a percentage of all live cells (7-AAD^-) in Figure 7C. We found that in MM.1S cells the percentage of live apoptotic cells increased with compound concentration, surpassing 20% at a 12.5 μM concentration. (Essentially no live cells were left after exposure to 25 μM I_{HSF}115.) In HeLa cells, an increase in live apoptotic cells could only be observed at 25 μM I_{HSF}115. We conclude that an apoptotic mechanism of cell death plays a far more important role in MM.1S cells than in HeLa cells. A cell cycle analysis corroborated the latter conclusion (Figure 7D). The percentage of MM.1S cells in sub-G0/G1 fractions rose to almost 13% (at 12.5 μM compound) after 6 h and to 43% (at 3.125 μM compound) after 15 h of exposure to I_{HSF}115. Thus, a large fraction of MM.1S cells was killed by apoptosis induced by I_{HSF}115. In contrast, only about 6% of HeLa cells exposed to 25 μM compound for 24 h were found in sub-G0/G1 fractions, suggesting that the large majority of these cells experienced death by a non-apoptotic mechanism.

DISCUSSION

It appears to be a widely held belief that transcription factors lacking a ligand-binding domain are essentially 'undruggable', i.e not specifically targetable by drug-like molecules (59,60). Nevertheless, there are rare examples where small-molecule drug candidates were successfully developed. In these cases, drugs were aimed at interrupting well-defined protein–protein interactions, e.g. the MDM2–p53 interaction (61). The approach that we have taken in this study appears to be unusual, or possibly unique, in that it did not target any known interaction between a transcription factor, here HSF1, and a co-factor. Instead, it consisted of a rational drug development program involving molecular modeling, identification of binding cavities, design of appropriate pharmacophores, assembly of a small library of lead-like compounds satisfying pharmacophore criteria and employment of a discriminating screening method to identify a lead compound that was subsequently improved by standard medicinal chemistry. That this approach yielded an inhibitor of HSF1 that is effective at high submicromolar/low micromolar concentrations, i.e. in a concentration range in which many approved drugs and drug candidates are active, should be encouraging. Our findings may catalyze the development of a novel cancer therapeutic. Concerning the many other not-liganded transcription factors that represent preferred therapeutic targets, the present study may give an indication that not all of them may be undruggable.

I_{HSF}115 does not interfere with heat-induced HSF1 oligomerization and HSE DNA binding. ChIP experiments showed that I_{HSF}115 also does not reduce HSF1 binding to intact chromatin. Hence, either nuclear import of HSF1 is not inhibited, or it is not of critical importance. However, apparent binding of HSF1 to chromatin was reduced by I_{HSF}058. This observation may be readily explained as a consequence of HSF1 degradation that this inhibitor causes. That the inhibitors do not affect HSF1 DNA binding is consistent with their design. Lead compound 001 from which they were derived was selected based on its expected ability to bind a pocket in the HSF1 DNA-binding domain that is not proximal to its DNA interaction region.

We note that minor differences in the structure of the inhibitors can result in significantly different effects on HSF1. I_{HSF}058 but not I_{HSF}115 induces degradation of the transcription factor. Apparently, the two compounds differently affect HSF1 conformation and/or access of protein cofactors.

Since I_{HSF}115 does not interfere with HSF1 binding to chromatin, the compound appears to regulate the transcriptional activity of the factor. We found that I_{HSF}115 inhibits binding of ATF1 to HSF1. Previous work had shown that ATF1 is a pivotal component of the transcription factor complexes that mediate HSF1 target gene transcription in heat-shocked cells (19). Interestingly, ATF1 interacts with a region within the DNA-binding domain of HSF1. This interaction may be weakened by a conformational change in the HSF1 DNA-binding domain induced by I_{HSF}115. Alternatively, the inhibitor may interfere directly with ATF1 docking by binding to the same or an adjacent site.

As I_{HSF}115 does not appear to affect heat stress signaling and does not inhibit heat-induced HSF1 DNA binding but transcription initiation, the inhibitor can be used to obtain a 'snapshot' of heat-induced or heat-repressed HSF1-mediated transcription. The inhibitor probes transcription when transcription factors including HSF1 are assembled on the genes and reveals the genes in which HSF1 control over transcription predominates. This view of the transcription process could not be obtained if I_{HSF}115 also inhibited HSF1 DNA binding. With HSF1 unable to bind, control over transcription of certain heat-regulated genes may be usurped by other transcription factors that are capable of conveying heat regulation (52), but which factors are normally subrogated to HSF1. An analogous situation may be created by HSF1 knockdown or genetic deletion.

When we analyzed the effects of heat treatment on the HeLa cell transcriptome, we observed that the majority (nearly 2/3) of heat-induced genes were inhibited by I_{HSF}115, i.e. were positively regulated by HSF1. All

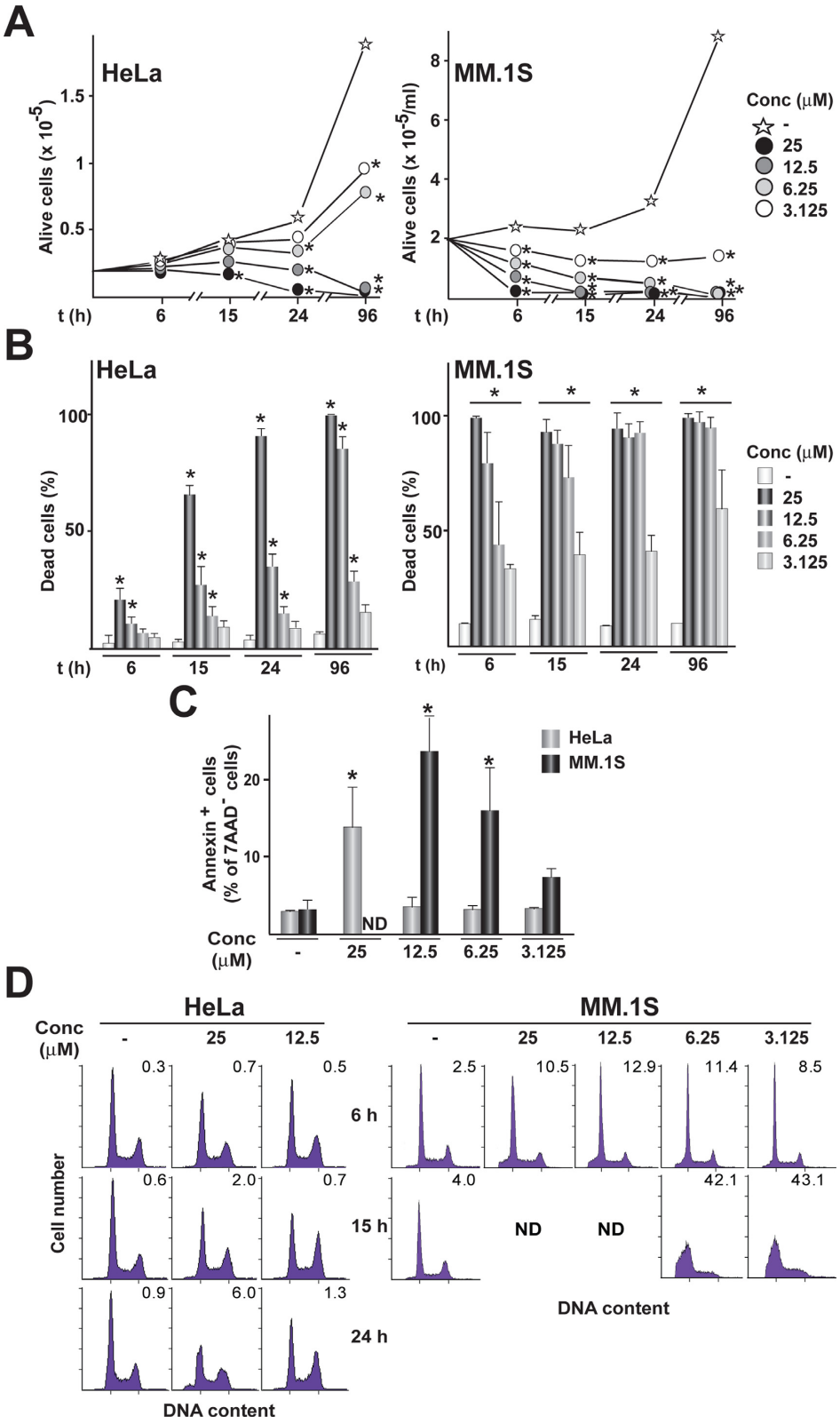

Figure 7. $I_{HSF}115$-induced cell death. (**A** and **B**) HeLa or MM.1S cells were exposed to the indicated concentrations of $I_{HSF}115$, or to vehicle (−), for 6, 15, 24 or 96 h. Trypan blue dye exclusion was used to determine numbers of alive cells (A) and percentages of necrotic cells (B). *$P < 0.05$; comparing to cells exposed to vehicle at each time point. (**C**) HeLa and MM.1S cells were exposed to the indicated concentrations of $I_{HSF}115$, or to vehicle (−), for 6 h and then double-stained with Annexin V-FITC and 7-AAD. Percentages of early apoptotic cells (Annexin V^+/7-AAD^-) are shown. *$P < 0.05$; comparing to the corresponding cell type exposed to vehicle. (**D**) DNA contents of HeLa or MM.1S cells that had been exposed to the indicated concentrations of $I_{HSF}115$, or to vehicle (−), for 6, 15 and 24 h. Percentages of apoptotic cells are indicated within the histograms.

genes for which a statistically significant effect of the inhibitor could not be obtained were counted as not regulated by HSF1 ('not-inhibited'). We noticed that the frequency of HSF1-inhibited versus not-inhibited genes decreased with decreasing heat inducibility, whereas the effectiveness of inhibition by $I_{HSF}115$ increased. We take this to reflect a limitation of the analysis. Small inhibitory effects can be expected to be increasingly unlikely to reach statistical significance as the differential between heat-induced and basal expression level decreases. Taking this into account, our extrapolation suggests that most heat-induced genes may be regulated by HSF1. Hence, our study suggests that HSF1 plays a predominant role in the transcription of heat-induced genes. Earlier studies had reached the opposite conclusion, i.e. that the large majority of heat-induced genes are not regulated by HSF1 (29,52). In the latter studies, absence of heat induction in cells in which HSF1 was knocked out or knocked down, respectively, was used as the criterion for deciding whether a heat-induced gene is HSF1-regulated. As discussed above, a reason for the difference in the number of genes considered HSF1-regulated between an HSF1 inhibitor-based study and a comparative analysis of HSF1-containing and HSF1-deficient cells may be that 'secondary' heat regulation of certain genes may take over in HSF1-deficient cells with the result that HSF1-regulated genes are missed. Establishment of such secondary regulation may be facilitated by various transcriptomic and/or metabolic adaptations that HSF1 knockdown or knockout cells may have undergone to compensate for the HSF1 deficiency. Consistent with this hypothesis is that many positively HSF1-regulated genes contain binding sites for transcription factors suggested to be capable of conferring heat regulation such SRF (about 60% of genes), and E2F2 (about 33% of genes), NFE2L2 (about 13% of genes), YY2 (about 57% of genes) and ELF1(about 60% of genes).

All studies agree that most of the heat-repressed genes are repressed by a mechanism that does not involve HSF1. For the minority of genes that are HSF1-regulated, repression was proposed to be brought about by HSF1 molecules binding to intragenic sites and obstructing progression of RNA polymerase (62,63). Recent evidence argues against such a mechanism: no accumulation of RNA polymerase could be detected upstream from intragenic HSF1 binding sites (52). Our finding that $I_{HSF}115$ prevents or attenuates the heat-induced repression of certain genes even though the compound does not interfere with HSF1 DNA binding is in keeping with the latter evidence. It would also appear to rule out the possibility that repression can be caused by HSF1 molecules binding to promoter regions and interfering with transcription initiation. Instead, it suggests that repression is mediated by transcriptionally active HSF1 molecules.

A consensus HSE sequence was defined for a subgroup of the positively HSF1-regulated genes identified in this study. Somewhat surprisingly, this consensus sequence was markedly degenerate when compared to a consensus sequence derived from a group of classical *HSP* genes or from HSF1-binding sites defined by ChIP-Seq (30). Thus, certain genes are heat-regulated by HSF1 despite containing only rudimentary HSEs. Stable binding of HSF1 to chromatin appears to require better defined HSEs. Barring technical explanations, these observations support a view that HSF1 is capable of directing transcription through subtle interactions with promoter DNA, which interactions may be stabilized and/or enhanced by other transcription factors and co-factors.

Cancer cells frequently exhibit a dependency on HSF1 activity for survival and proliferation as was first demonstrated in the pioneering study of Dai *et al*. (31). In the same study, the cytotoxic effect of HSF1 depletion by siRNA was examined in a panel of human cancer cell lines, of which some were also present in the panel tested in the present study (Figure 6B). Sensitivity to HSF1 depletion (by hA6 shRNA) decreased in the following order: HeLa > T47D > MDA-MB-231 > MCF-7 > PC-3/BT-20 > BT-474. In the present study, the order was MDA-MB-231 > PC-3 > T47D > MCF-7/BT-474 > HeLa > BT-20 (Figure 6B). Based on this limited sample of cell lines, it would appear that cancer cell lines respond differently to HSF1 depletion and HSF1 inhibition. For example, HeLa cells are highly sensitive to HSF1 depletion but not to HSF1 inhibition. While there may be multiple possible reasons for these differences in responsiveness, one that is difficult not to consider is that inhibition involves an acute drop in HSF1 activity while depletion is a process that occurs over many hours/days. The slow process of HSF1 depletion may allow for transcriptomic and/or metabolic changes in cancer cells that mitigate or enhance the cytotoxic effect of loss of HSF1 activity, which changes may not occur upon abrupt disruption of HSF1 function.

After the work reported herein had been completed, structural information on human HSF1 and HSF2 became available (PDB entries and refs. 64,65). HSF1 crystal structures 5D5U, 5D5V and the NMR structure of 2LDU show a cavity in a similar position to that of cavity A in our homology model. Admittedly, the cavities in 5D5U and 5D5V have a slightly different shape to our homology model, and it may be difficult for the docking program to give a potential pose for the hit molecules against these new crystal structures. However, the 2LDU NMR structure has 20 different conformations that adhere to the NMR data, showing the residues which line the pocket can be modeled in different positions. Given that a number of protein conformations can be generated that satisfy the NMR data, we believe that more conformations are potentially available and that (our model of) cavity A represents a feasible conformation that can be considered. There may also be an element of 'induced fit' where the protein could respond to the presence of an I_{HSF}. From the 5D5U and 5D5V crystal structures, we believe that cavity A is accessible when HSF1 is complexed with DNA. It is noted that the pocket is also present in the HSF2 crystal structures 5D8K and 5D8L, but again its shape is slightly different when compared with the HSF1 crystal structures, although this pocket may be able to change dynamically. Consequently, it is not inconceivable that I_{HSF} could also target HSF2.

SUPPLEMENTARY DATA

Supplementary Data are available at NAR Online.

ACKNOWLEDGEMENTS

To the memory of our colleague and friend Dr Luis Alvarez, Head of the Molecular Hepatology Group at IdiPAZ, who left us on 6 July 2016. The authors thank Jesus García and Pedro Botias (Unidad de Genómica–Universidad Complutense de Madrid/Parque Científico de Madrid, Spain) (microarray analyses), Dr Ricardo Ramos and Silvia Vazquez (Unidad de Genómica–Universidad Autónoma de Madrid/Parque Científico de Madrid) (TaqMan gene expression studies) as well as Prof. Maria José Hernaiz and Dr Juan Treviño (Universidad Complutense de Madrid) (SPR analysis) for their assistance. Prof. Dermot Walls (Dublin City University, Ireland) kindly provided *pGSLink*.

FUNDING

HSF Pharmaceuticals SA; Ministry of Economy and Competitiveness (MINECO), Spain [SAF2013-50364-EXP]; Instituto de Salud Carlos III-Fondos FEDER, MINECO [PI15/01118]; Program I2 of the Autonomous Community of Madrid, Spain (to N.V.). Funding for open access charge: HSF Pharmaceuticals SA.

Conflict of interest statement. HSF Pharmaceuticals and the Foundation for Biomedical Research of the La Paz University Hospital claim rights to the I_{HSF} disclosed herein.

REFERENCES

1. Richter,K., Haslbeck,M. and Buchner,J. (2010) The heat shock response: life on the verge of death. *Mol. Cell*, **40**, 253–266.
2. Hartl,F.U., Bracher,A. and Hayer-Hartl,M. (2011) Molecular chaperones in protein folding and proteostasis. *Nature*, **475**, 324–332.
3. Ananthan,J., Goldberg,A.L. and Voellmy,R. (1986) Abnormal proteins serve as eukaryotic stress signals and trigger the activation of heat shock genes. *Science*, **232**, 522–524.
4. Hightower,L.E. (1980) Cultured animal cells exposed to amino acid analogues or puromycin rapidly synthesize several polypeptides. *J. Cell. Physiol.*, **102**, 407–427.
5. McMillan,D.R., Xiao,X., Shao,L., Graves,K. and Benjamin,I.J. (1998) Targeted disruption of heat shock transcription factor 1 abolishes thermotolerance and protection against heat-inducible apoptosis. *J. Biol. Chem.*, **273**, 7523–7528.
6. Akerfelt,M., Morimoto,R.I. and Sistonen,L. (2010) Heat shock factors: integrators of cell stress, development and life span. *Nat. Rev. Mol. Cell Biol.*, **11**, 545–555.
7. Zou,J., Guo,Y., Guettouche,T., Smith,D.O. and Voellmy,R. (1998) Repression of heat shock transcription factor HSF1 by Hsp90 (Hsp90 complex) that forms a stress-sensitive complex with HSF1. *Cell*, **94**, 471–480.
8. Ali,A., Bharadwaj,S., O'Carroll,R. and Ovsenek,N. (1998) Hsp90 interacts with and regulates the activity of heat shock factor 1 in *Xenopus* oocytes. *Mol. Cell. Biol.*, **18**, 4949–4960.
9. Duina,A.A., Kalton,H.M. and Gaber,R.F. (1998) Requirement for Hsp90 and a Cyp-40-type cyclophilin in negative regulation of the heat shock response. *J. Biol. Chem.*, **273**, 18974–18978.
10. Voellmy,R. and Boellmann,F. (2007) Chaperone regulation of the heat shock protein response. *Adv. Exp. Med. Biol.*, **594**, 89–99.
11. Dai,Q., Zhang,C., Wu,Y., McDonough,H., Whaley,R.A., Godfrey,V., Li,H.H., Madamanchi,N., Xu,W., Neckers,L. *et al.* (2003) CHIP activates HSF1 and confers protection against apoptosis and cellular stress. *EMBO J.*, **22**, 5446–5458.
12. Boyault,C., Zhang,Y., Fritah,S., Caron,C., Gilquin,B., Kwon,S.H., Garrido,C., Yao,T-P., Vourc'h,C., Matthias,P. *et al.* (2007) HDAC6 controls major cell response pathways to cytotoxic accumulation of protein aggregates. *Genes Dev.*, **21**, 2172–2181.
13. Pernet,L., Faure,V., Gilquin,B., Dufour-Guérin,S., Khochbin,S. and Vourc'h,C. (2014) HDAC6-ubiquitin interaction controls the duration of HSF1 activation after heat shock. *Mol. Biol. Cell*, **25**, 4187–4194.
14. Boellmann,F., Guettouche,T., Guo,Y., Fenna,M., Mnayer,L. and Voellmy,R. (2004) DAXX interacts with heat shock factor 1during stress activation and enhances its transcriptional activity. *Proc. Natl. Acad. Sci. U.S.A.*., **101**, 4100–4105.
15. Wang,X.Z., Grammatikakis,N., Siganou,A., Stevenson,M.A. and Calderwood,S.K. (2004) Interactions between extracellular signal-regulated protein kinase 1, 14-3-3e, and heat shock factor 1 during stress. *J. Biol. Chem.*, **279**, 49460–49469.
16. Hu,Y. and Mivechi,N.F. (2011) Promotion of heat shock factor Hsf1 degradation via adaptor protein filamin A-interacting protein 1-like (FILIP-1L). *J. Biol. Chem.*, **286**, 31397–31408.
17. Satyal,S.H., Chen,D., Fox,S.G., Kramer,J.M. and Morimoto,R.I. (1998) Negative regulation of the heat shock transcriptional response by HSBP1. *Genes Dev.*, **12**, 1962–1974.
18. Fujimoto,M., Takaki,E., Takii,R., Tan,K., Prakasam,R., Hayashida,N., Iemura,S.-I., Natsume,T. and Nakai,A. (2012) RPA assists HSF1 access to nucleosomal DNA by recruiting histone chaperone FACT. *Mol. Cell*, **48**, 182–194.
19. Takii,R., Fujimoto,M., Tan,K., Takaki,E., Hayashida,N., Nakato,R., Shirahige,K. and Nakai,A. (2015) ATF1 modulates the heat shock response by regulating the stress-inducible heat shock factor 1 transcription complex. *Mol. Cell. Biol.*, **35**, 11–25.
20. Rabindran,S.K., Haroun,R.I., Clos,J., Wisniewski,J. and Wu,C. (1993) Regulation of heat shock factor trimer formation: role of a conserved leucine zipper. *Science*, **259**, 230–234.
21. Guo,Y., Guettouche,T., Fenna,M., Boellmann,F., Pratt,W.B., Toft,D.O., Smith,D.F. and Voellmy,R. (2001) Evidence for a mechanism of repression of heat shock factor 1 transcriptional activity by a multichaperone complex. *J. Biol. Chem.*, **276**, 45791–45799.
22. Shi,Y., Mosser,D.D. and Morimoto,R.I. (1998) Molecular chaperones as HSF1-specific transcriptional repressors. *Genes Dev.*, **12**, 654–666.
23. Guettouche,T., Boellmann,F., Lane,W.S. and Voellmy,R. (2005) Analysis of phosphorylation of human heat shock factor 1 in severely heat-stressed cells. *BMC Biochem.*, **6**, 4.
24. Chou,S.-D., Prince,T., Gong,J. and Calderwood,S.K. (2012) mTOR is essential for the proteotoxic stress response, HSF1 activation and heat shock protein synthesis. *PLoS One*, **7**, e39679.
25. Hietakangas,V., Ahlskog,J.K., Jakobsson,A.M., Hellesuo,M., Sahlberg,N.M., Holmberg,C.I., Mikhailov,A., Palvimo,J.J., Pirkkala,L. and Sistonen,L. (2003) Phosphorylation of serine 303 is a prerequisite for the stress-inducible SUMO modification of heat shock factor 1. *Mol. Cell. Biol.*, **23**, 2953–2968.
26. Raychaudhuri,S., Loew,C., Körner,R., Pinkert,S., Theis,M., Hayer-Hartl,M., Buchholz,F. and Hartl,F.U. (2014) Interplay of acetyltransferase EP300 and the proteasome system in regulating heat shock transcription factor 1. *Cell*, **156**, 975–985.
27. Westerheide,S.D., Anckar,J., Stevens,S.M. Jr, Sistonen,L and Morimoto,R.I. (2009) Stress-inducible regulation of heat shock factor 1 by the deacetylase SIRT1. *Science*, **323**, 1063–1066.
28. Trinklein,N.D., Murray,J.I., Hartman,S.J., Botstein,D. and Myers,R.M. (2004) The role of heat shock transcription factor 1 in the genome-wide regulation of the mammalian heat shock response. *Mol. Biol. Cell*, **15**, 1254–1261.
29. Page,T.J., Sikder,D., Yang,L., Pluta,L., Wolfinger,R.D., Kodadek,T. and Thomas,R.S. (2006) Genome-wide analysis of human HSF1 signaling reveals a transcriptional program linked to cellular adaptation and survival. *Mol. Biosyst.*, **2**, 627–639.
30. Mendillo,M.L., Santagata,S., Koeva,M., Bell,G.W., Hu,R., Tamimi,R.M., Fraenkel,E., Ince,T.A., Whitesell,L. and Lindquist,S. (2012) HSF1 drives a transcriptional program distinct from heat shock to support highly malignant human cancers. *Cell*, **150**, 549–562.
31. Dai,C., Whitesell,L., Rogers,A.B. and Lindquist,S. (2007) Heat shock factor 1 is a powerful multifaceted modifier of carcinogenesis. *Cell*, **130**, 1005–1018.
32. Zhao,Y.H., Zhou,M., Liu,H., Ding,Y., Khong,H.T., Yu,D., Fodstad,O. and Tan,M. (2009) Upregulation of lactate dehydrogenase A by ErbB2 through heat shock factor 1 promotes breast cancer cell glycolysis and growth. *Oncogene*, **28**, 3689–3701.

33. Ciocca,D.R., Arrigo,A.P. and Calderwood,S.K. (2013) Heat shock proteins and heat shock factor 1 in carcinogenesis and tumor development: an update. *Arch. Toxicol.*, **87**, 19–48.
34. Khaleque,M.A., Bharti,A., Sawyer,D., Gong,J., Benjamin,I.J., Stevenson,M.A. and Calderwood,S.K. (2005) Induction of heat shock proteins by heregulin β1 leads to protection from apoptosis and anchorage-independent growth. *Oncogene*, **24**, 6564–6573.
35. Nakamura,Y., Fujimoto,M., Hayashida,N., Takii,R., Nakai,A. and Muto,M. (2010) Silencing HSF1 by short hairpin RNA decreases cell proliferation and enhances sensitivity to hyperthermia in human melanoma cell lines. *J. Derm. Sci.*, **60**, 187–192.
36. Meng,L., Gabai,V.L. and Sherman,M.Y. (2010) Heat-shock transcription factor HSF1 has a critical role in human epidermal growth factor receptor-2-induced cellular transformation and tumorigenesis. *Oncogene*, **29**, 5204–5213.
37. Gabai,V.L., Meng,L., Kim,G., Mills,T.A., Benjamin,I.J. and Sherman,M.Y. (2012) Heat shock transcription factor Hsf1 is involved in tumor progression via regulation of hypoxia-inducible factor 1 and RNA-binding protein HuR. *Mol. Cell. Biol.*, **32**, 929–940.
38. Santagata,S., Hu,R., Lin,N.U., Mendillo,M.L., Collins,L.C., Hankinso,S.E., Schnitt,S.J., Whitesell,L., Tamimi,R.M., Lindquist,S. *et al.* (2011) High levels of nuclear heat-shock factor 1 (HSF1) are associated with poor prognosis in breast cancer. *Proc. Natl. Acad. Sci. U.S.A.*, **108**, 18378–18383.
39. Yoon,Y.J., Kim,J.A., Shin,K.D., Shin,D.-S., Han,Y.M., Lee,Y.J., Lee,J.S., Kwon,B.-M. and Han,D.C. (2011) KRIBB11 inhibits Hsp70 synthesis through inhibition of heat shock factor 1 function by impairing the recruitment of positive transcription elongation factor b to the hsp70 promoter. *J. Biol. Chem.*, **286**, 1737–1747.
40. Yoon,S.J., Lee,S.W., Kim,N.D., Park,Y.K., Lee,G.H., Kim,J.W., Park,S.J., Park,H.J. and Shin,D.H. (2001) Novel 3-nitropyridine derivatives and the pharmaceutical composition containing said derivatives. *International Patent Application Publication WO 01/38306, May 31 2001*.
41. Salamanca,H.H., Antonyak,M.A., Cerione,R.A., Shi,H. and Lis,J.T. (2014) Inhibiting heat shock factor 1 in human cancer cells with a potent RNA aptamer. *PLoS One*, **9**, e96330.
42. Vilaboa,N., Fenna,M., Munson,J., Roberts,S.M. and Voellmy,R. (2005) Novel gene switches for targeted and timed expression of proteins of interest. *Mol. Ther.*, **12**, 290–298.
43. Zuo,J., Baler,R., Dahl,G. and Voellmy,R. (1994) Activation of the DNA-binding ability of human heat shock transcription factor 1 may involve the transition from an intramolecular to an intermolecular triple-stranded coiled-coil structure. *Mol. Cell. Biol.*, **14**, 7557–7568.
44. Zuo,J., Rungger,D. and Voellmy,R. (1995) Multiple layers of regulation of human heat shock transcription factor 1. *Mol. Cell. Biol.*, **15**, 4319–4330.
45. Loughran,S.T., Loughran,N.B., Ryan,B.J., D'Souza,B.N. and Walls,D. (2006) Modified His-tag fusion vector for enhanced protein purification by immobilized metal affinity chromatography. *Anal. Biochem.*, **355**, 148–150.
46. Goldenberg,C.J., Luo,Y., Fenna,M., Baler,R., Weinmann,R. and Voellmy,R. (1988) Purified human factor activates heat shock promoter in a HeLa cell-free transcription system. *J. Biol. Chem.*, **263**, 19734–19739.
47. Vilaboa,N.E., Calle,C., Pérez,C., De Blas,E., García-Bermejo,L. and Aller,P. (1995) cAMP increasing agents prevent the stimulation of heat-shock protein 70 (HSP70) gene expression by cadmium chloride in human myeloid cell lines. *J. Cell Sci.*, **108**, 2877–2893.
48. Huang,D.W., Sherman,B.T. and Lempicki,R.A. (2009) Systematic and integrative analysis of large gene lists using David bioinformatics resources. *Nat. Protoc.*, **4**, 44–57.
49. Ritchie,M.E., Phipson,B., Wu,D., Hu,Y., Law,C.W., Shi,W. and Smyth,G.K. (2015) limma powers differential expression analyses for RNA-sequencing and microarray studies. *Nucleic Acids Res.*, **43**, e47.
50. Mahalingam,P., Takrouri,K., Chen,T., Sahoo,R., Papadopoulos,E., Chen,L., Wagner,G., Aktas,B.H., Halperin,J.A. and Chorev,M. (2014) Synthesis of rigidified eIF4E/eIF4G inhibitor-1 (4EGI-1) mimetic and their in vitro characterization as inhibitors of protein-protein interaction. *J. Med. Chem.*, **57**, 5094–5111.
51. Jones,G., Willet,P. and Glenh,R.C. (1995) Molecular recognition of receptor sites using a genetic algorithm with a description of desolvation. *J. Mol. Biol.*, **245**, 43–53.
52. Mahat,D.B., Salamanca,H.H., Duarte,F.M., Danko,C.G. and Lis,J.T. (2016) Mammalian heat shock response and mechanisms underlying its genome-wide transcriptional regulation. *Mol. Cell*, **62**, 63–78.
53. Vihervaara,A., Sergelius,C., Vasara,J., Blom,M.A., Elsing,A.N., Roos-Mattjus,P. and Sistonen,L. (2013) Transcriptional response to stress in the dynamic chromatin environment of cyclin and mitotic cells. *Proc. Natl. Acad. Sci. U.S.A.*, **110**, E3388–E3397.
54. Sandqvist,A., Björk,J.K., Akerfelt,M., Chitikova,Z., Frichine,A., Vourc'h,C., Jolly,C., Salminen,T.A., Nymalm,Y. and Sistonen,L. (2009) Heterotrimerization of heat shock factors 1 and 2 provides a transcriptional switch in response to distinct stimuli. *Mol. Biol. Cell*, **20**, 1340–1347.
55. He,H., Soncin,F., Grammatikakis,N., Li,Y., Siganou,A., Gong,J., Brown,S.A., Kingston,R.E. and Calderwood,S.K. (2003) Elevated expression of heat shock factor (HSF) 2A stimulates HSF1-induced transcription during stress. *J. Biol. Chem.*, **278**, 35465–35475.
56. Oestling,P., Björk,J.K., Roos-Mattjus,P., Mezger,V. and Sistonen,L. (2007) Heat shock factor 2 (HSF2) contributes to inducible expression of *hsp* genes through interplay with HSF1. *J. Biol. Chem.*, **282**, 7077–7086.
57. Logan,I.R., McNeil,H.V., Cook,S., Lu,X., Meek,D.W., Fuller-Pace,F.V., Lunec,J. and Robson,C.N. (2009) Heat shock factor-1 modulates p53 activity in the transcriptional response to DNA damage. *Nucleic Acids Res.*, **37**, 2962–2971.
58. Hideshima,T., Richardsom,P., Chaudhan,D., Palombella,V.J., Elliott,P.J., Adams,J. and Anderson,K.C. (2001) The proteasome inhibitor PS-341 inhibits growth, induces apoptosis and overcomes drug resistance in human multiple myeloma cells. *Cancer Res.*, **61**, 3071–3076.
59. Darnell,J.E. Jr (2002) Transcription factors as targets for cancer therapy. *Nat. Rev. Cancer*, **2**, 740–749.
60. Vazquez,A., Bond,E.E., Levine,A.J. and Bond,G.L. (2008) The genetics of the p53 pathway, apoptosis and cancer. *Nat. Rev. Drug Discov.*, **7**, 979–987.
61. Zhao,Y., Bernard,D. and Wang,S. (2013) Small molecule inhibitors of MDM2-p53 and MDMX-p53 interactions as new cancer therapeutics. *Biodiscovery*, **8**, 4.
62. Westwood,J.T., Clos,J. and Wu,C. (1991). Stress-induced oligomerization and chromosomal relocalization of heat-shock factor. *Nature*, **353**, 822–827.
63. Guertin,M.J. and Lis,J.T. (2010). Chromatin landscape dictates HSF binding to target DNA elements. *PLoS Genet.*, **6**, e1001114.
64. Neudegger,T., Verghese,J., Hayer-Hartl,M., Hartl,F.U. and Bracher,A. (2016) Structure of human heat-shock transcription factor 1 in complex with DNA. *Nat. Struct. Mol. Biol.*, **23**, 140–146.
65. Jaeger,A.M., Pemble,C.W., Sistonen,L. and Thiele,D.J. (2016) Structures of HSF2 reveal mechanisms for differential regulation of human heat-shock factors. *Nat. Struct. Mol. Biol.*, **23**, 147–154.